

Quarterly Report, Volume II

PLANETARY SOLAR ARRAY DEVELOPMENT

Prepared for  
Jet Propulsion Laboratory  
California Institute of Technology  
4800 Oak Grove Drive  
Pasadena, California  
Attention: M. Beckstrom

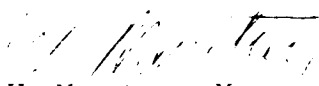
Contract 952035

EOS Report 7254-Q-3

15 April 1968

Prepared by  
R. Wizenick, Program Manager

Approved by

  
W. Menetrey, Manager  
Space Electronics Division

This work was performed for the Jet Propulsion  
Laboratory, California Institute of Technology,  
as sponsored by the National Aeronautics and  
Space Administration under Contract No. NAS7-100.



**ELECTRO - OPTICAL SYSTEMS, INC.**  
A XEROX COMPANY

# ABSTRACT

This is the third quarterly report describing the work completed at EOS of the Planetary Solar Array Development Study Program, JPL contract 952035.

This report finalizes the requirements of Task III and is presented in three volumes.

PRECEDING PAGE BLANK NOT FILMED.

## CONTENTS

1.	INTRODUCTION	1-1
2.	PACKAGING AND DEPLOYMENT	2-1
	2.1 Packaging	2-1
	2.2 Deployment	2-9
3.	ELECTROCAL ANALYSIS	3-1
	3.1 Solar Cells	3-1
	3.2 Solar Cell Covering	3-2
	3.3 Solar Cell Radiation Degradation	3-10
	3.4 Circuit Design	3-17
	3.5 Electrical Power Analysis	3-17
	3.6 Magnetic Field Analysis	3-34
	3.6.1 Sun at the Zenith of the Spacecraft	3-39
	3.6.2 Sun-Shade Condition	3-39
	3.6.3 Conclusion	3-45
4.	STRUCTURAL DESIGN AND ANALYSIS	4-1
	4.1 Substrate	4-1
	4.1.1 Description	4-1
	4.1.2 Material Selection	4-2
	4.1.3 Mathematical Models	4-2
	4.1.4 Critical Load Analysis	4-2
	4.1.5 Stress Analysis	4-5
	4.2 Structure	4-8
	4.2.1 Rotating Boom	4-8
	4.2.2 Support Truss	4-12
5.	SYSTEM ANALYSIS	5-1
	5.1 Environmental Interaction	5-1
	5.2 Materials Evaluation	5-1
	5.3 Thermal Analysis - Flat Panels	5-1
	5.4 Weight Analysis, Two Panel Oriented Array	5-4

## CONTENTS (contd)

5.5	Reliability Considerations for the Two Axis Horizontally Mounted Array	5-4
5.5.1	Physical Description	5-4
5.5.2	Reliability Definition	5-4
5.5.3	Power Capability	5-7
5.5.4	Failure Mode Discussion	5-7
6.	PRELIMINARY MANUFACTURING PLAN	6-1
6.1	Facilities	6-1
6.1.1	Location	6-1
6.1.2	Whiteroom Facilities	6-2
6.1.3	Storage Areas	6-2
6.1.4	Resident Offices	6-3
6.2	Manufacturing Flow Plan	6-3
6.2.1	Incoming Cell Test and Matching	6-3
6.2.2	Submodule Fabrication	6-5
6.2.3	Module Series Strings	6-5
6.2.4	Substrate Fabrication	6-6
6.2.5	Handling Procedures	6-6
6.2.6	Module Bonding to Substrate	6-7
6.3	Material Status Control	6-7
6.4	Document Preparation and Its Use	6-10
7.	PRELIMINARY TEST PLAN	7-1
7.1	Introduction	7-1
7.1.1	Definitions	7-1
7.2	Solar Array Tests	7-2
7.2.1	Engineering Evaluation Test	7-2
7.2.2	Prototype Testing	7-4
7.2.3	Acceptance Test	7-5
7.2.4	Qualification Test	7-6

CONTENTS (contd)

7.2.5	Formal Type Approval Test	7-6
7.2.6	Reliability Test	7-9
7.2.7	Shipping Container Test	7-10
7.3	Test Equipment and Fixtures	7-10
7.4	Performance Testing	7-11
7.4.1	Single Cell Testing	7-11
7.4.2	Submodule Testing	7-11
7.4.3	Sample Module Testing	7-11
7.4.4	Panel Testing	7-12
8.	SUMMARY	8-1

## SECTION 1

### INTRODUCTION

This report is Volume II of three volumes of the third quarterly report. It represents the detailed study of the two-panel-oriented solar array.

## SECTION 2

### PACKAGING AND DEPLOYMENT

This section details the mechanical packaging and deployment of a photovoltaic power system having sun tracking capabilities and which consists basically of two solar panels which are mounted universally on each end of a main, centrally located horizontal boom.

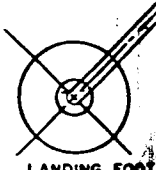
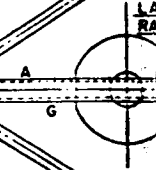
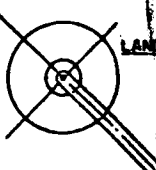
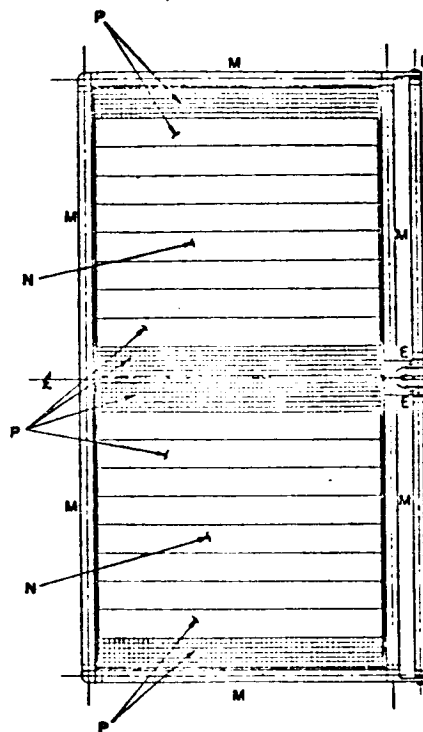
The two panel oriented solar array, as well as support and deployment elements, is depicted on Electro-Optical Systems Drawing Number 7254-116, Fig. 2-1, which includes a legend for identification of the various mechanical and structural elements of this system. This design provides for the solar panels being mounted on opposite sides of the spacecraft in such a manner that the other two spacecraft sides are always completely unobstructed, and there is no interference with the vehicle antenna system.

#### 2.1 PACKAGING

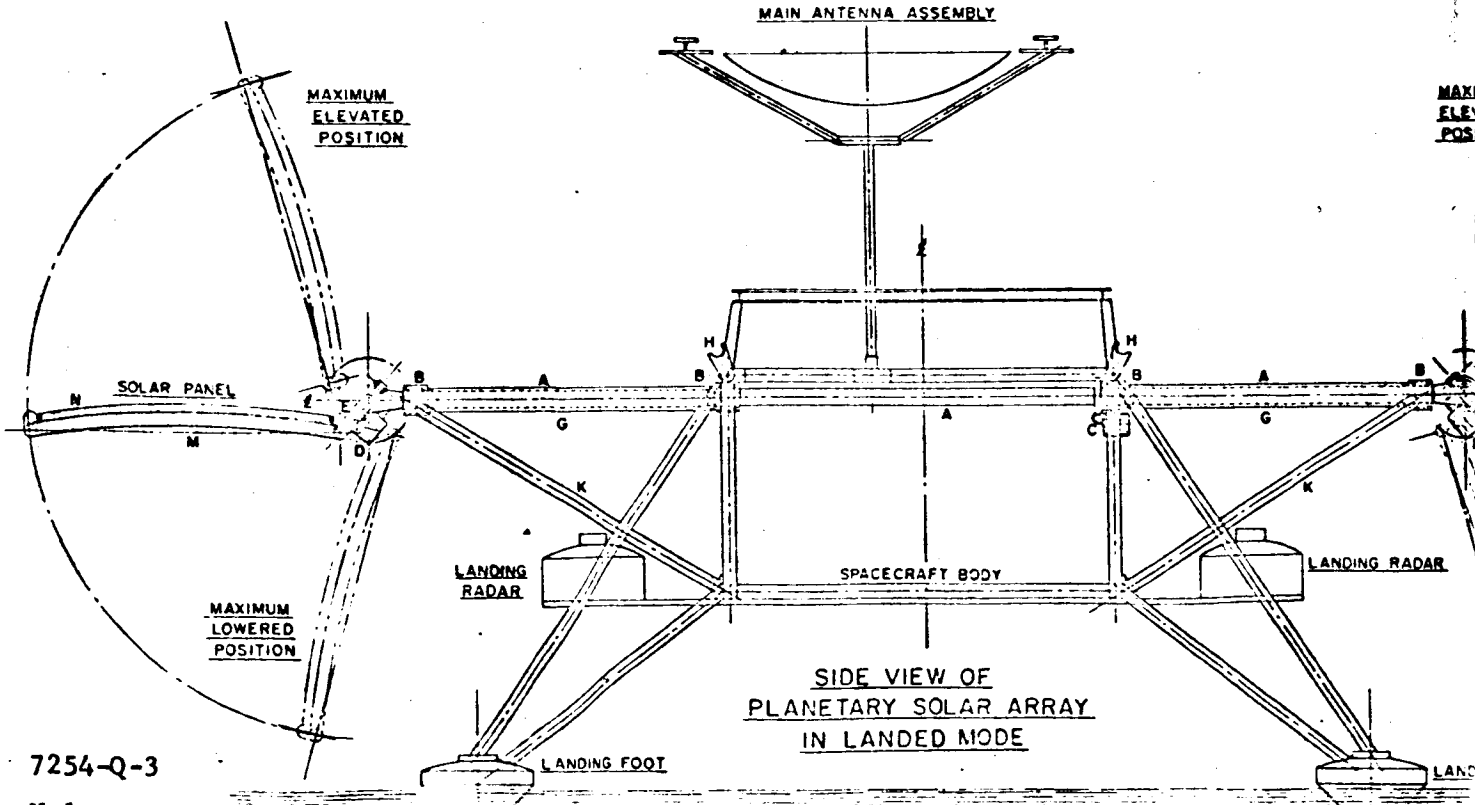
The following is a discussion of the mechanical aspects for a conceptual design of a photovoltaic power system which meets the design constraints of Jet Propulsion Laboratory Drawing Number 1002-3236 A, and Electro-Optical Systems Drawing Number 7254-100, Fig. 2-2. It provides for solar cell circuits being permanently affixed to one side only of the substrate of each of two equal sized array panels. For convenience in manufacture and testing, the two equal sized array panels are again divided into two segments. Each segment is in the form of an aluminum hollow core substrate with integral beryllium tubing frames around its periphery. Two such segments, when bonded and bolted together, form one solar panel which is one-half of the complete power system. The

SECURITY CLASSIFICATION

NOTED: UNLESS OTHERWISE SPECIFIED



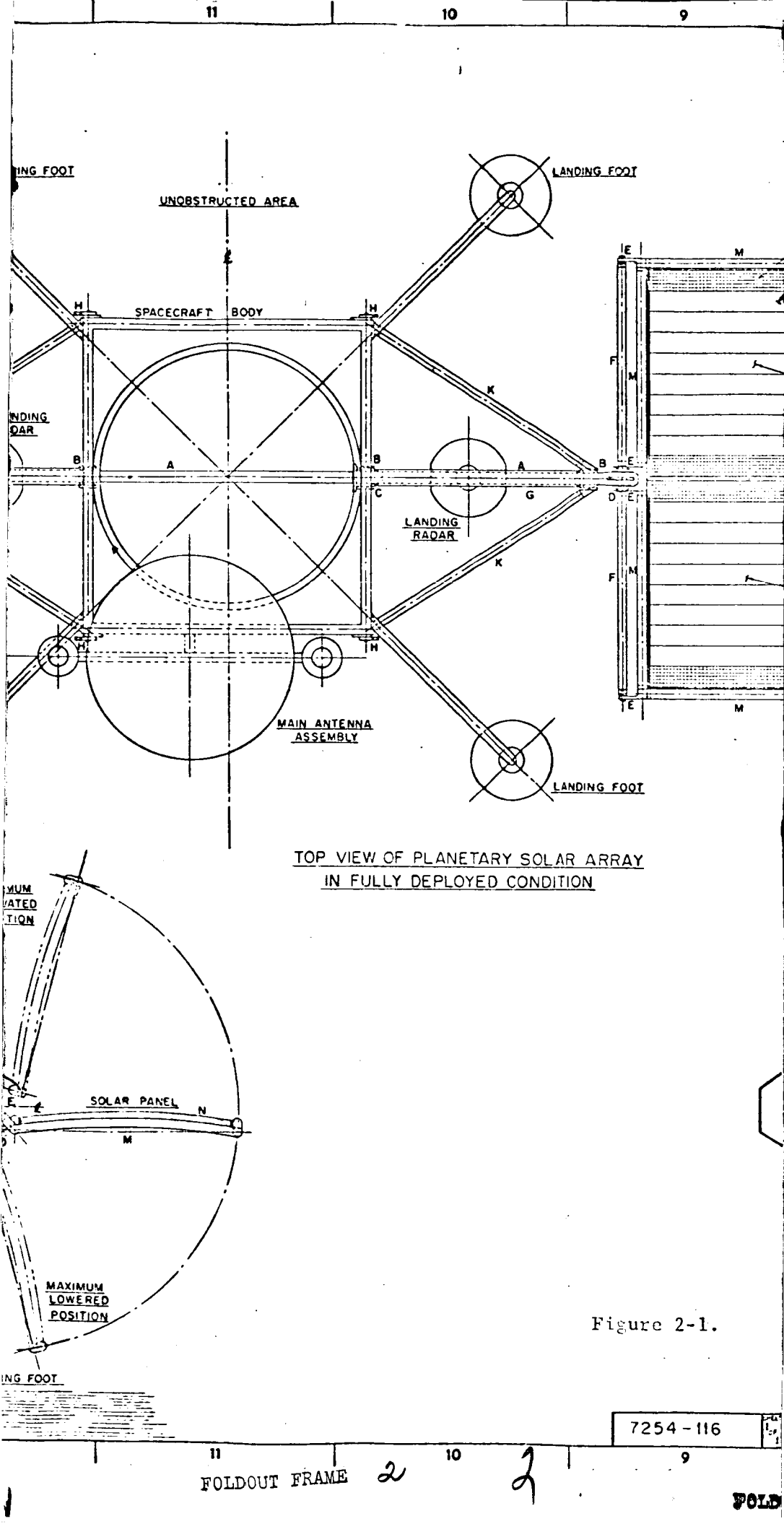
LANDING FOOT

MAXI  
ELEV  
POS

7254-Q-3

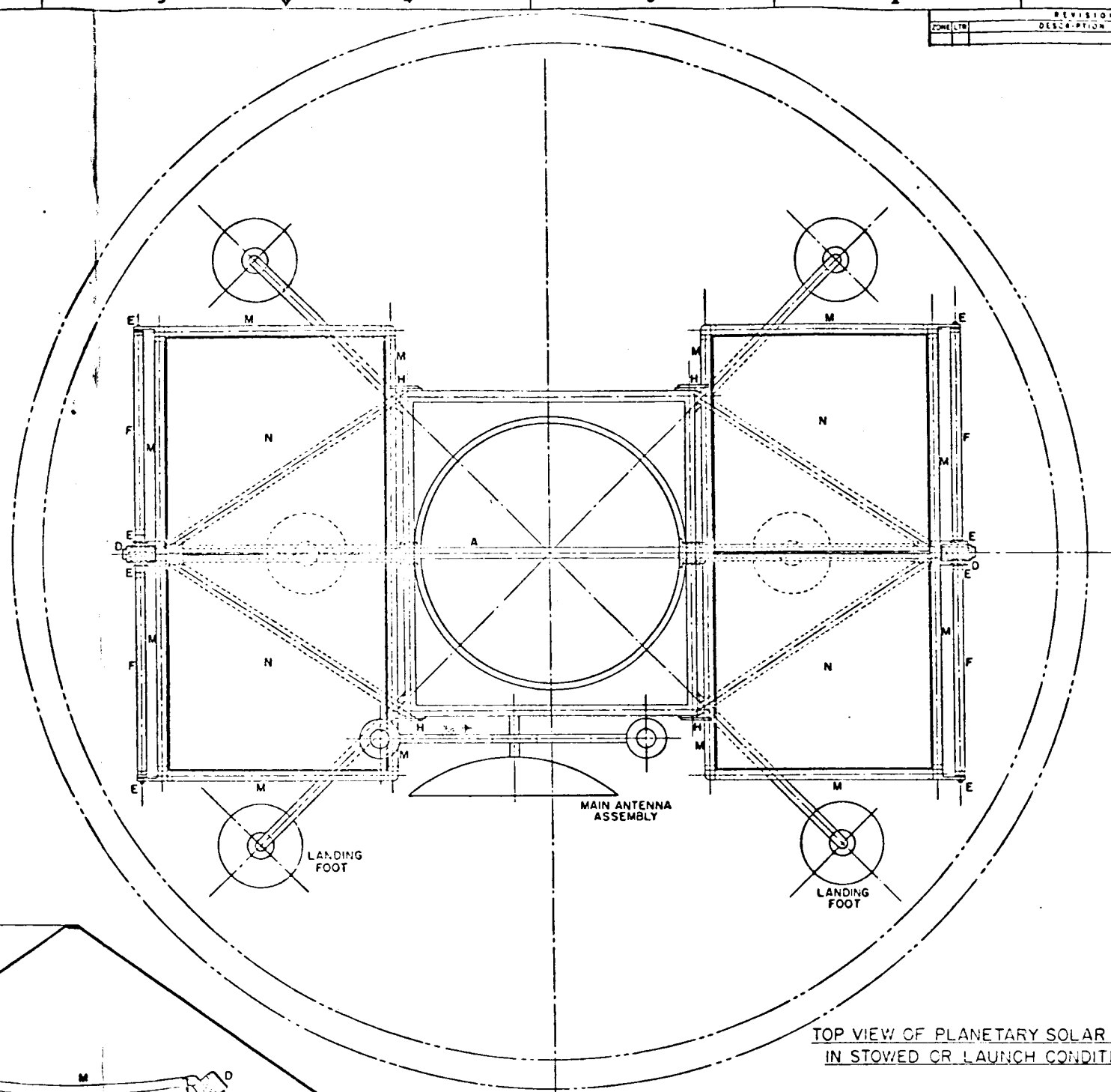
Volume II



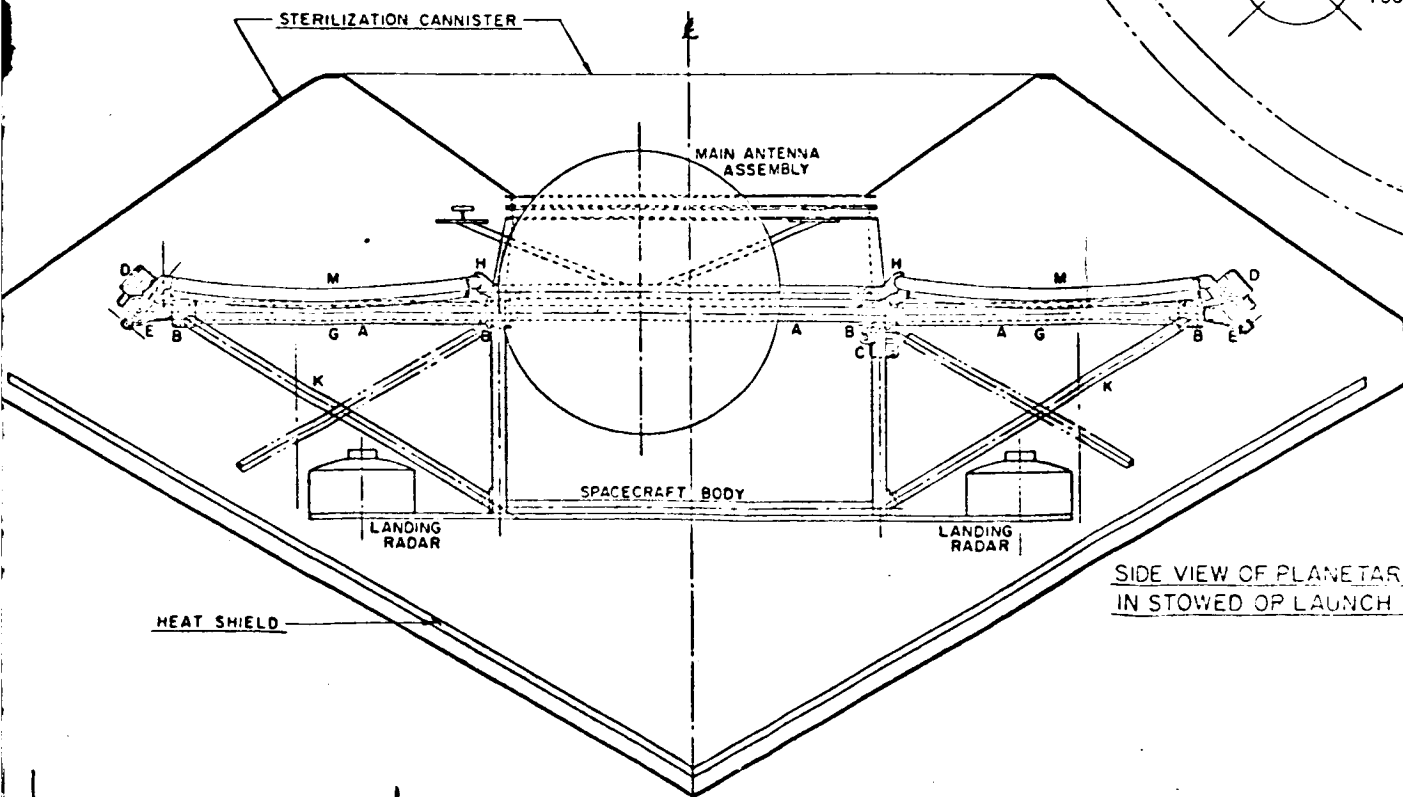


# LEGEND

- A-HORIZONTAL BOOM
- B-HORIZONTAL BOOM BEARINGS
- C-BOOM ROTATING DRIVE MECHANISM
- D-ARRAY DEPLOYMENT DRIVE MECHANISM
- E-ARRAY DEPLOYMENT PIVOT HINGES
- F-PIVOT HINGE SHAFT
- G-BEARING SPACER AND BOOM HOUSING
- H-LAUNCH MODE LATCHES
- K-MAIN SUPPORT TRUSS
- M-SOLAR ARRAY FRAME
- N-SOLAR CELL SUBSTRATE
- P-SOLAR CELL CIRCUIT



TOP VIEW OF PLANETARY SOLAR ARRAY  
IN STOWED OR LAUNCH CONDITION



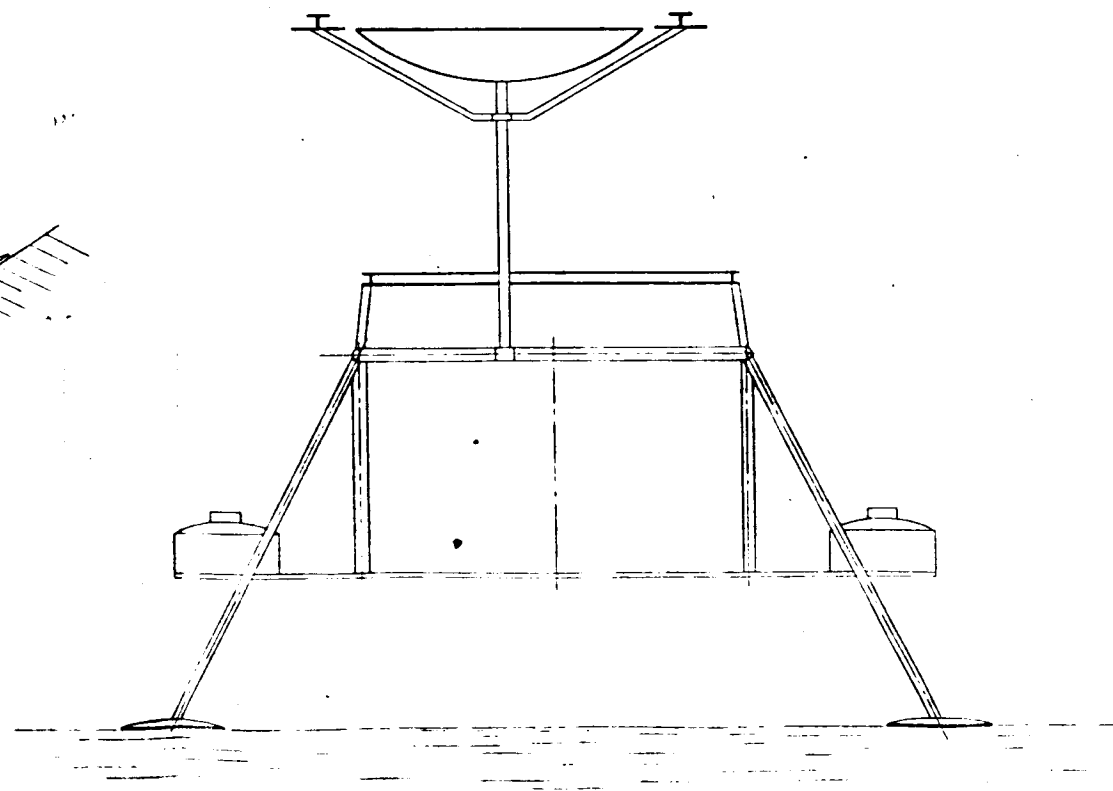
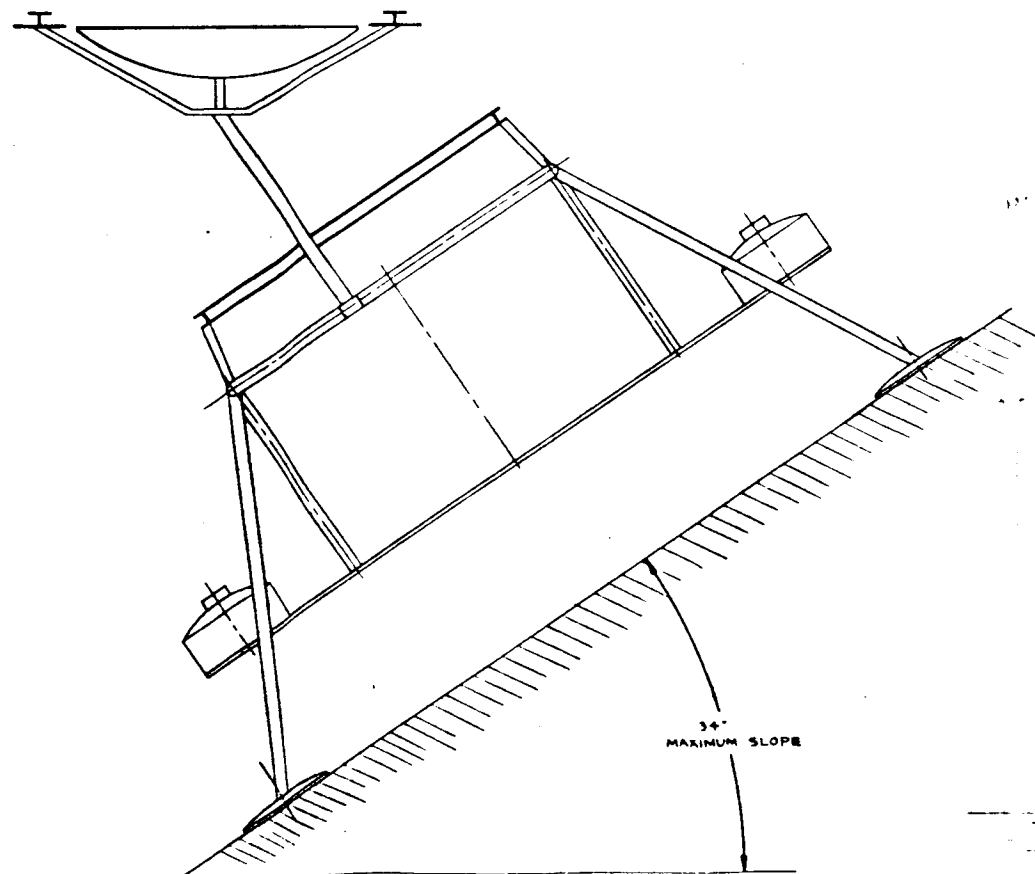
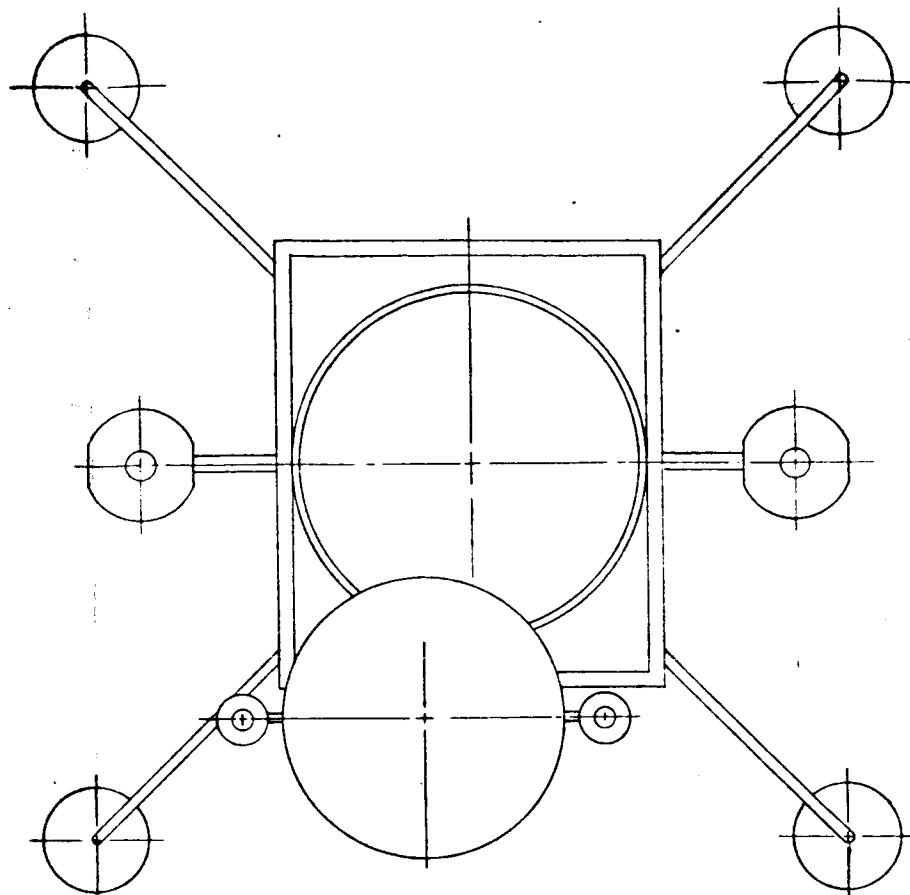
SIDE VIEW OF PLANETARY SOLAR ARRAY  
IN STOWED OR LAUNCH CONDITION

0 10 20 30 40 50 60 70 80 90 100  
SCALE IN INCHES

QTY	SYM	CODE	IDENT	PART OR IDENT	NO	HOW MANY OF OR	MATERIAL	SPECIFICATION	UNIT	ZONE	ITEM
LIST OF MATERIALS											
ELECTRO-OPTICAL SYSTEMS, INC.											
A PERIOD COMPANY											
TITLE PLANETARY SOLAR ARRAY -											
TWO AXIS ORIENTATION -											
HORIZONTAL BOOM DESIGN											
DATE 12/70											
J 12705 7254-116											
SCALE 1/2" = 1'-0"											
SHEET 1 OF 1											

SECURITY CLASSIFICATION

NOTES

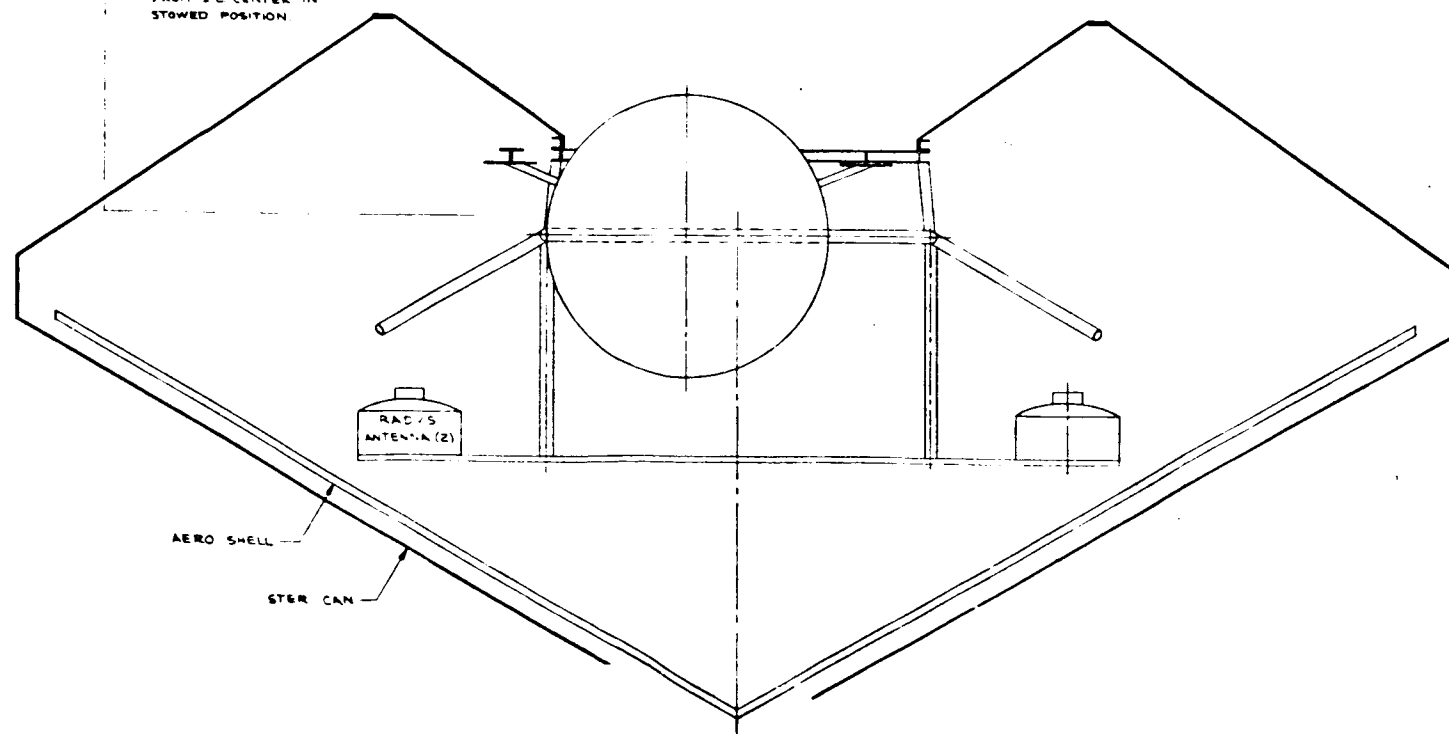
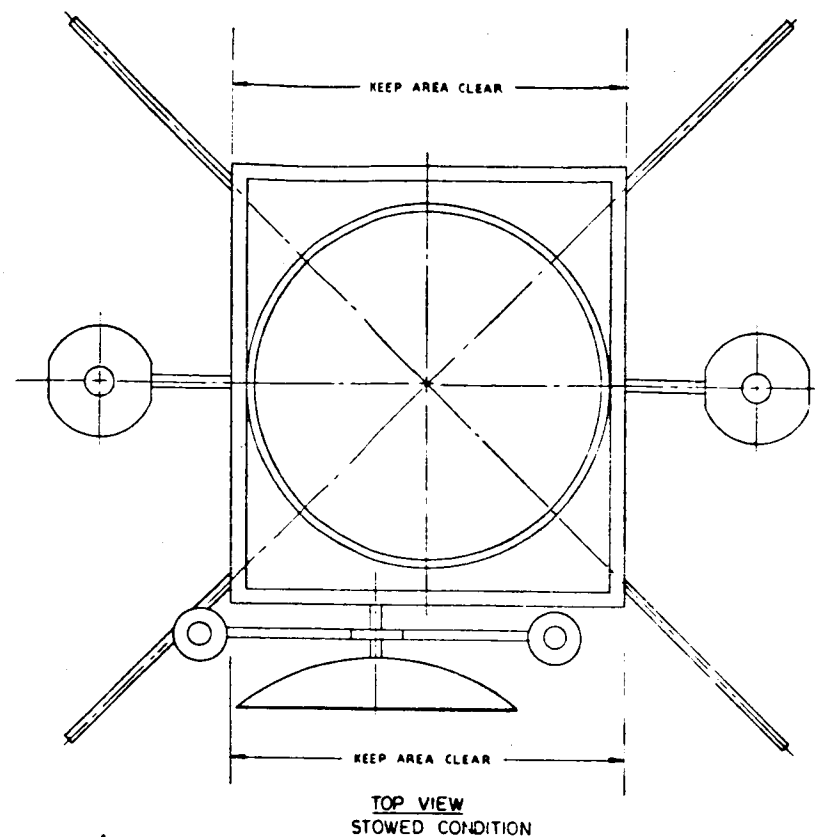


EXTENDED POSITION

7254-Q-3  
Volume II

7254-10C

REVISIONS			
NO.	DESCRIPTION	DATE	APPROVED



SIDE VIEW  
STOWED CONDITION

SCALE - INCHES  
0 10 20 30 40 50 60

QTY REQD	SYM	CODE IDENT	PART OR IDENTIFYING NO	NOMENCLATURE OR DESCRIPTION	MATERIAL	SPECIFICATION	UNIT WT	ZONE	ITEM NO
<p>UNLESS OTHERWISE NOTED LINEAR DIMS IN INCHES TOLERANCES DECIMAL FRACTIONAL FINISH ANGULAR DIMENSIONS DO NOT SCALE</p>									
<p>CONTRACT NO. DATE DRAWN BY CHECKED BY DESIGN MATERIAL TREATMENT FINISH DESIGN ACTIVITY APPD S. MILAR TO ACT WT SCALE WT CUSTOMER</p>									
<p>ON THE EFFECTIVE SERIAL NO. NO. PER ALLOC. APPLICATION DRAWING LEVEL</p>									
<p>LIST OF MATERIALS ELECTRO-OPTICAL SYSTEMS, INC. A Subsidiary of Aero Corporation 800 N. Main Street, Pasadena, California, 91107 TITLE: LAYOUT - SOLAR PANEL CLEARANCE SCALE: 1/2" = 1'-0" J 12705 7254-100 SCALE: 1/2" = 1'-0" RELEASE DATE SHEET 1 OF 1</p>									

FOLDOUT FRAME

FOLDOUT FRAME

two solar panels will be mounted into the sterilization canister in a horizontal position on two opposite sides of the spacecraft and securely latched to the spacecraft body during the launch and flight mode.

The main support structure for the two solar panels consists of a Horizontal Boom, A, which is common to the two panels and passes completely through the spacecraft body on its centerline. The outboard ends of the horizontal boom are braced by sets of Main Support Trusses, K. These truss assemblies are set in the form of A frames and are mounted in a slanting condition from the extreme ends of the boom to the four bottom corners of the spacecraft. The outboard slanting ends of the two support trusses are tied back to the top of the spacecraft body by Stationary Tubes, G, which are coaxial with the horizontal boom and serve the additional purpose of being the spacers between the inboard and outboard main bearings.

The horizontal boom is free to rotate about its own axis and is supported at both extreme ends, and also at the points where it enters the sides of the main spacecraft body, by means of four Horizontal Boom Bearings, B. The horizontal boom is a 2.0 inch diameter, thin-wall beryllium tube which is bonded to specially designed lightweight metal end and center fittings. These end and center fittings provide the mating surfaces for the inner races of the four main bearings. The rotational motion of the horizontal boom is applied and controlled by means of the Boom Rotating Drive Mechanism, C, which is located at one side of the spacecraft body. This is composed of a gearmotor whose output is from a worm into a worm gear which is mounted on the main bearing fitting of the horizontal boom.

A special end fitting on each end of the horizontal boom is also provided with a worm gear for the movement and sun-tracking capabilities

of the two solar panels, whose motion is at 90 degrees to that of the rotational motion of the horizontal boom. The solar panel motion is accomplished by means of a gearmotor located on the center hinge assembly of each panel. The output of these gearmotors is from a worm around the worm gears which are stationarily located in the special end fittings of the horizontal boom. This provides for the two panel moving gearmotors to ride with the panels on the center hinge assembly of each, with the capability of moving the two solar panels independently of each other. These panel motors are designated as Array Deployment Drive Mechanism, D, on the reference drawing and receive their drive input from solar sensors which are located at both ends of their respective solar panels.

The outboard ends of the two solar panels are supported during rotation, and also in any stationary position, by means of special outboard hinges which are located on the end fittings of the two Pivot Hinge Shafts, F. The pivot hinge shafts are composed of 2.0 inch diameter thin-wall beryllium tubing with lightweight metal end fittings which include necessary bearing retainers for the hinges.

The two solar panels which are located on opposite ends of the horizontal boom comprise the complete Photovoltaic Power System. Each solar panel contains one half of the solar circuits of the total system and each panel is designed to operate independently, both mechanically and electrically, of the other. The substrates, to which the solar circuits are bonded, are composed of aluminum hollow core in a biconvex mode. The substrates are bonded to the Solar Array Frames, M, which are composed of 2.0 inch diameter thin-wall beryllium tubing with lightweight metal end fittings and hinge fittings.

During the launch mode, or stowed condition, the two half-sections of the completely assembled and tested solar power system will be folded

inward toward the spacecraft body and will be securely latched in four places by means of the Launch Mode Latches, H. Unlatching will be accomplished pyrotechnically.

## 2.2 DEPLOYMENT

After landing, deployment of the two half-sections of the solar array will be accomplished in either a sequential or a simultaneous manner immediately after the erection of the main antenna assembly. Deployment will be from a preprogrammed system to unlatch from the stowed condition, and may be activated by a programmer aboard the spacecraft or from earth command.

The same program, or earth command, will then rotate the horizontal boom and position the two solar panels so that they "find" the sun. After proper initial positioning, the two panels will "lock onto the sun" by means of paralleled solar sensing devices which are located on both ends of each solar panel. The two panels will continue to track the sun throughout the Martian day, at the end of which they will be returned to the "sunrise condition" by either the programmer or earth command.

## SECTION 3

### ELECTRICAL ANALYSIS

This section details the electrical analysis for the two panel oriented solar array.

#### 3.1 SOLAR CELLS

The solar cells selected for this array are discussed in the 2nd quarterly report, No. 7254-Q-2. A solar cell of N/P type silicon with a bulk resistivity of 1-3 ohm-cm has been selected. Cells of this type are capable of producing more power in a relatively radiation-free environment than cells of a nominal 10 ohm-cm bulk resistivity range. The optimum cell thickness to minimize the solar array area and allow the maximum specific wt/sq ft to the substrate was determined in the 15 December report, and is 0.010 inch thick. EOS has chosen a solar cell of a top contact configuration. The advantage of a cell of this type is that it can be readily adapted to a series-parallel matrix submodule array. In addition, all the solder joints are visible on the top surface after bonding to the panel substrate, and the design allows close packaging of the individual cells yielding a smaller overall circuit configuration. The replacement of an individual cell, in the event of accidental damage, can be readily accomplished, and the back surface of the solar cell submodules are flat, and unincumbered with a connector and solder joints. This allows a minimum adhesive thickness to bond the cells to the substrate. EOS has elected to stay with the 2 x 2 cm cell size, even though the cover glass has been eliminated, for reliability considerations and to obtain more flexibility in the circuit. The cell specifications are:



- a. Type - N/P silicon
- b. Contacts - sintered silver-titanium
- c. Size - 2 x 2 cm
- d. Thickness - 0.010  $\pm$  0.001 inch
- e. Configuration - front contact (solderless)
- f. Resistivity - 1-3 ohm-cm
- g. Electrical output - 58 mW at 485 mV (28°C, AMO)

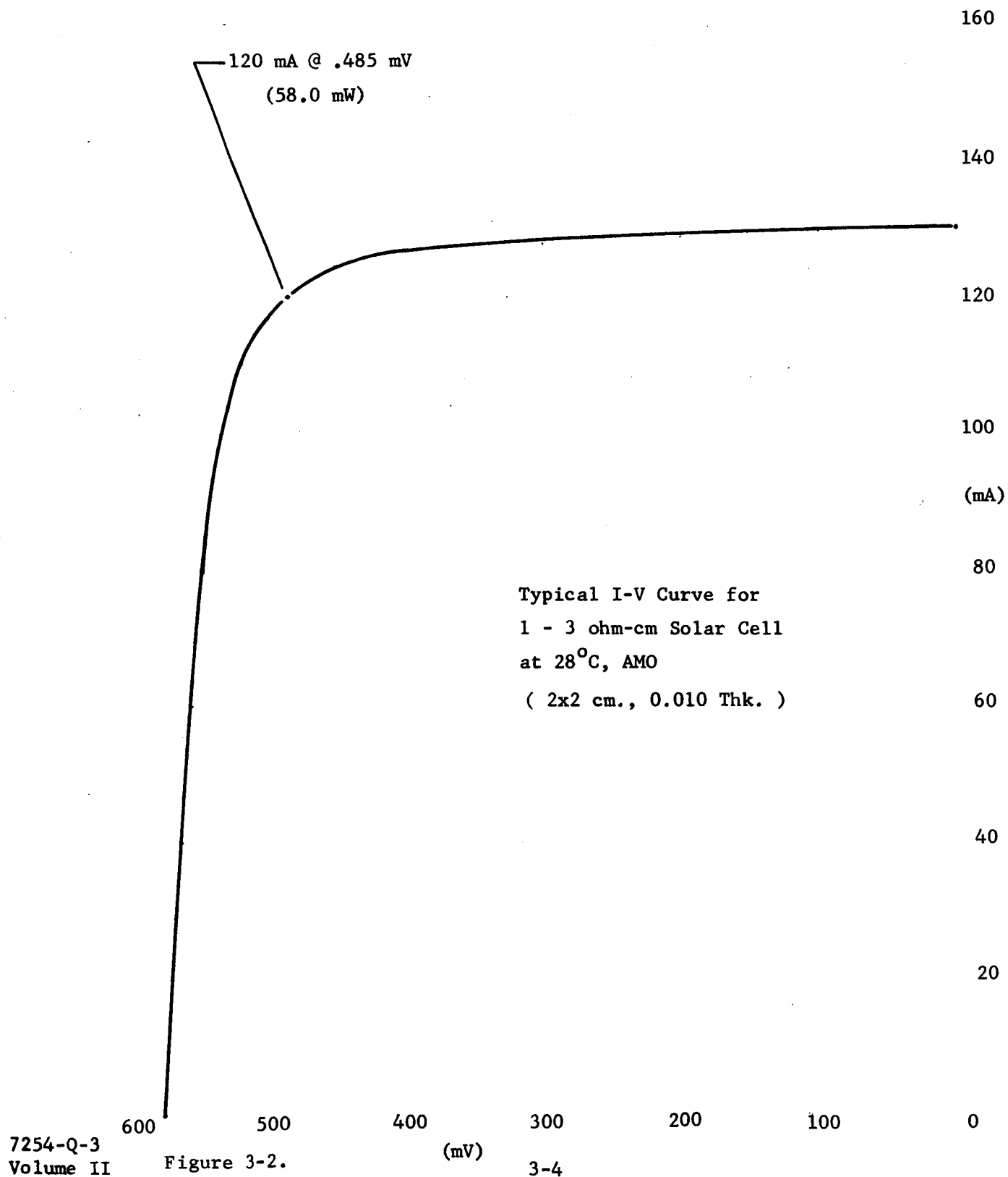
The cell is shown in EOS Drawing No. 7254-105, Fig. 3-1. A typical I-V curve of a cell of this type is shown in Fig. 3-2.

### 3.2 SOLAR CELL COVERING

Solar cell covers, or filters, of glass or fused silica have been used to enhance the emittance properties of solar arrays for many years. It has been empirically determined that 0.001 inch of either material is sufficient to yield the properties of the bulk materials. The filters also act as a shield to protect the cells from radiation degradation. The thickness of the filter is varied to suit the anticipated needs of the particular array. The radiation environment on the Martian surface is very low when compared to near earth environments, and this, coupled with the weight requirements of this mission, dictate the use of as thin a filter as practical. An 0.003 inch filter was first considered for the mission requirements.

However, a solar cell circuit operating on the Martian surface has a problem which is unique and not found in space applications. Mars has a dust condition which is considered severe; the dust is assumed to be iron oxide and electrically conductive. The electrical shorting caused by the dust would be catastrophic to the solar array. A study of the dust conditions on the Martian surface was made and reported in the first quarterly report. For reference, the electrical resistivity of iron oxide, in comparison with other known insulators, is as shown below:





<u>Material</u>	<u>Electrical Resistance (ohm-cm) at 300°K</u>
1. 99.24 Fe <sub>2</sub> O <sub>3</sub> and 0.76 Ti <sub>1</sub> O <sub>2</sub>	2
2. 99.85 Fe <sub>2</sub> O <sub>3</sub> and 0.15 TiO <sub>2</sub>	60
3. BeO	10 <sup>11</sup>
4. Al <sub>2</sub> O <sub>3</sub>	> 10 <sup>13</sup>
5. H-film (Kapton)	10 <sup>14</sup>

These data indicate that no electrical connections should be exposed.

One approach to this problem, which was considered, was to coat all electrically exposed areas of the solar cell circuit with filter adhesive. This approach has been used on solar panels for earth terrestrial applications. This method is tedious, virtually impossible to guarantee complete protection, and will add considerable weight to the solar array.

A second consideration was discussed in the 2nd quarterly report, that is, eliminating the cover glass and using a semiorganic resin developed by Dr. Burnn Marks of Lockheed Missiles and Space Company, Palo Alto, California. This coating has been developed specifically as a solar cell coating and can be applied by spraying techniques. This coating has been tested on solar cells for emissivity and light transmission, as well as for environmental space effects including ultraviolet, vacuum, electron irradiation, and temperature extremes. The principal drawback to this coating technique is the inability to completely insulate all electrically conducting surfaces. Spray application of the coating would not insulate the back side of connector tab, and dipping the total array is highly impractical. A heavy brush coating could be applied and techniques developed to remove the excess before curing. However, the material is not suited for this type of application.

EOS would like to propose a method for insulating the solar array by encapsulating the cells with a continuous sheet of DuPont Tedlar PVF film. Tedlar film is essentially transparent to, and unaffected by, solar radiation in the near ultraviolet, visible and near infrared regions of the spectrum. The transmission characteristics of transparent Tedlar film are shown in Figs. 3-3 and 3-4. One of the outstanding characteristics of Tedlar film is its resistance to solar degradation. Test samples of transparent film have not discolored and still retain 50% of their initial tensile strength after 10 years of outdoor weathering in Florida, facing south at 45° to the horizontal. Typical properties of Tedlar film Type 30 are:

- |                                  |                             |
|----------------------------------|-----------------------------|
| a. Tensile strength              | - 13,000 psi                |
| b. Yield point                   | - 5,000 psi                 |
| c. Density                       | - 1.38 g/cc                 |
| d. Refractive index              | - 1.467                     |
| e. Melting point                 | - > 300°C                   |
| f. Service temperature           | - 70°C to +105°C            |
| g. Coefficient thermal expansion | - $2.8 \times 10^{-5}$ (°F) |
| h. Dielectric strength           | - 3,500 V/mil               |
| i. Volume resistivity            | - $10^{14}$ ohm-cm          |

No previous data are available for the a/e properties of a solar cell covered with Tedlar film and filter adhesive. These measurements should be made under the Phase II portion of the program. The a/e value will probably lie somewhere between that of a bare cell and a filtered cell.

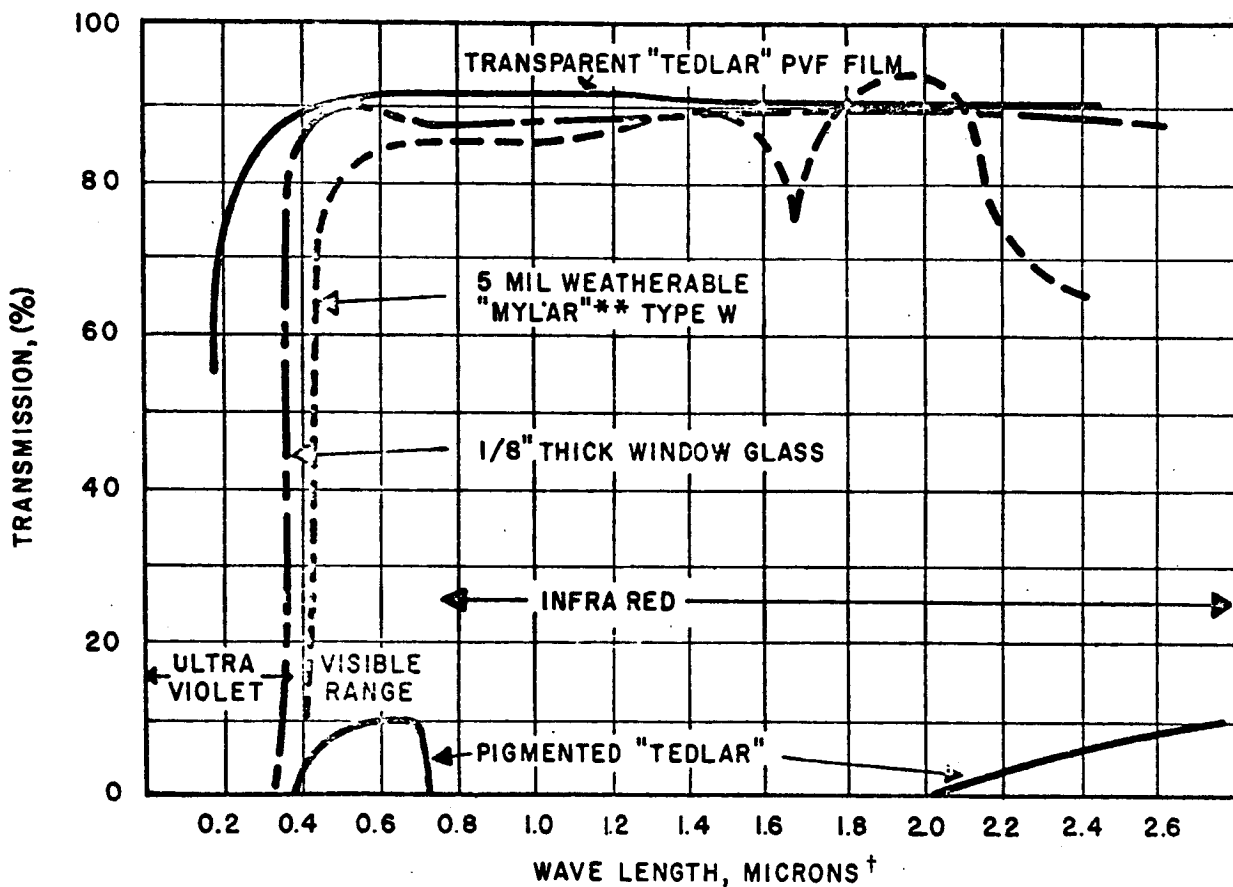
Electrical measurements of a solar cell, "filtered" with 1 mil type 30 transparent Tedlar film, and Dow Corning type XR-6-3489 silicone adhesive, and the I-V curve of a coated cell are shown in Fig. 3-5. The degradation percent at the maximum power point is:

# OPTICAL PROPERTIES

## SPECTRAL TRANSMISSION

Transparent types of "Tedlar"\* are essentially transparent to, and unaffected by, solar radiation in the near ultraviolet, visible and near infrared regions of the spectrum.

Transmission spectra for "Tedlar" are shown in Fig. 3-4.



\*Du Pont registered trademark for its PVF film

\*\*Du Pont registered trademark for its polyester film

NOTE (†) 10,000 Angstroms = 1 Micron = 0.001 mm

Figure 3-3.

"TEDLAR" INFRARED SPECTRUM

"Tedlar" PVF Film Type 50 SG20TR

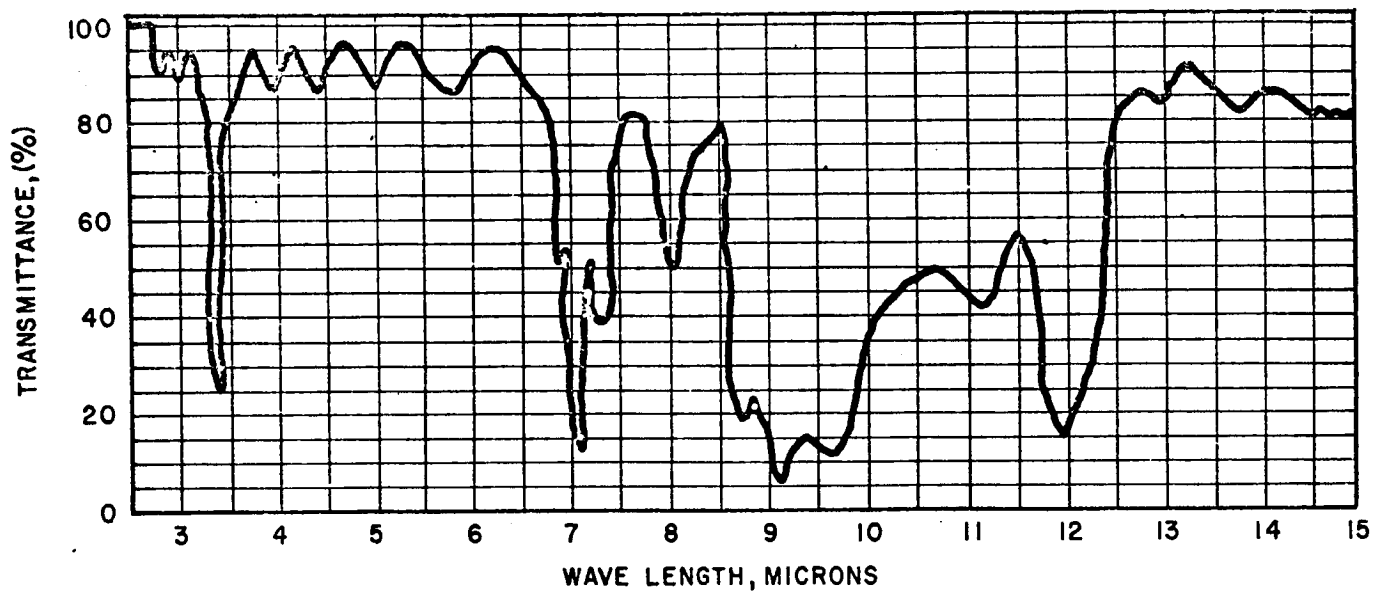
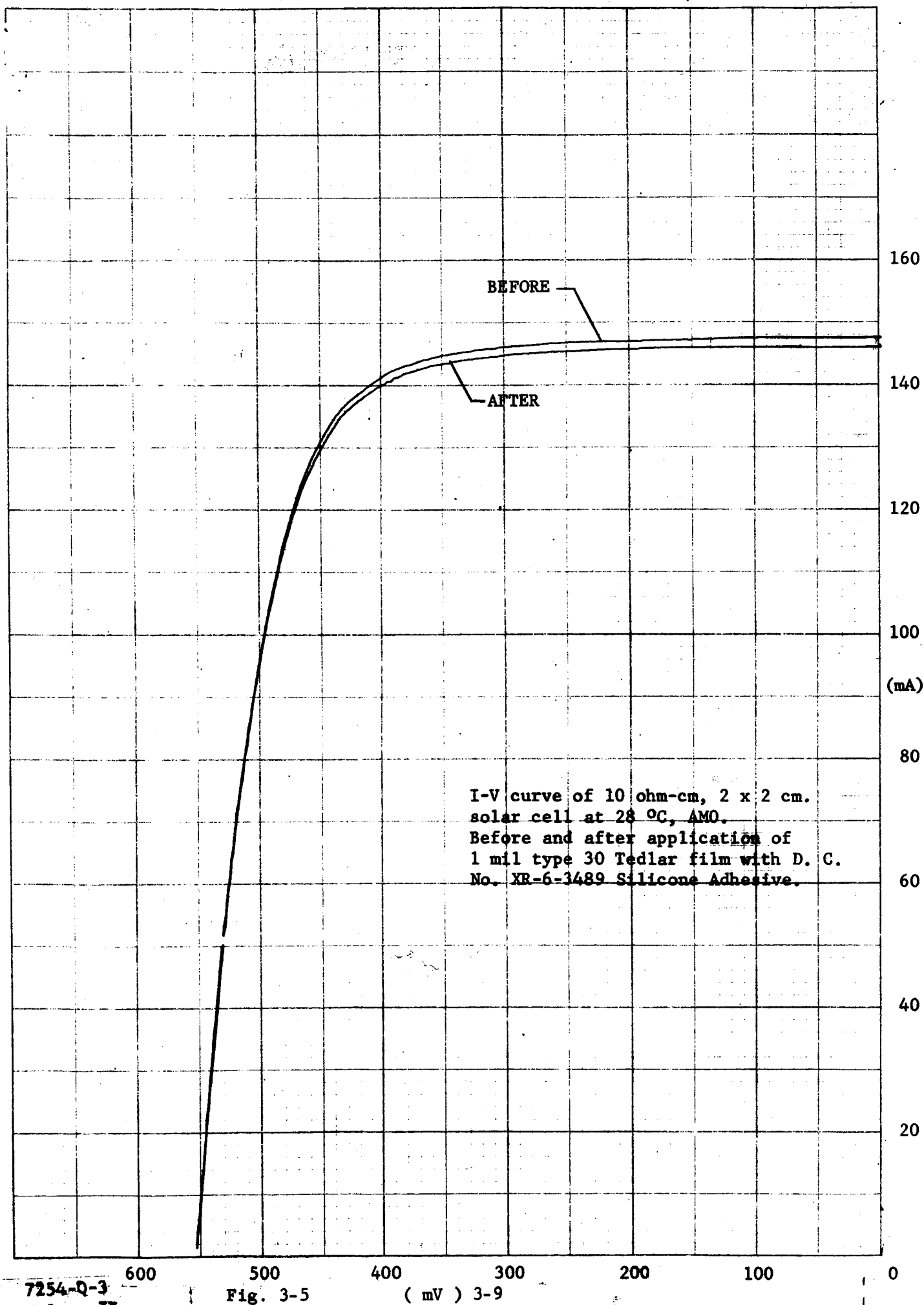


Figure 3-4.





$$\% = \frac{(136.5 - 135.5)}{136.5} \times 100$$

$$= 0.73\%$$

The degradation of less than 1% is comparable to losses experienced with quartz filters and significantly better than that experienced with microsheet filters.

The advantages of the film coating for the solar cell circuit are:

- a. Total insulation of all electrical conducting surfaces
- b. Low electrical loss due to coating
- c. Material is readily available
- d. Installation is easily accomplished using a space proven adhesive system
- e. Finished coating eliminates gaps between cells, which would form a trap for dust accumulation
- f. The coating will provide protection for the cells from low energy proton radiation, as the cells will have no exposed areas common to typically filtered cells
- g. The film is low in weight
- h. The flexible film, bonded with a resilient adhesive should have better abrasion resistance to the 'sandblasting effect' of the dust than the hard surface of glass or quartz filters

### 3.3 SOLAR CELL RADIATION DEGRADATION

The radiation that the solar array will be exposed to while operating on the Martian surface will be ultraviolet radiation from the sun spectrum, and proton radiation as a result of solar flares.

The ultraviolet radiation will not affect the Tedlar film or the silicone adhesive used to bond the film to the cell.

The intensity of the solar flare radiation for the planetary array mission in 1973 is based on the information provided in the JPL Voyager Environmental Predictions Document SE-003BB01-1B28, Paragraph III, D.4 Table 13 as shown below:

MAXIMUM TIME-INTEGRATED SOLAR FLARE FLUXES

	Energy (MeV)	Flux (protons/cm <sup>2</sup> ) (11 gm/cm <sup>2</sup> )
Maximum time-integrated proton flux/flare	E > 10	$1.2 \times 10^8$
	E > 30	$9.8 \times 10^7$
	E > 100	$6.7 \times 10^7$
Maximum time-integrated proton flux/year	E > 10	$1.6 \times 10^8$
	E > 30	$1.3 \times 10^8$
	E > 100	$9.3 \times 10^7$

Quantitative data for proton damage to silicon solar cells is relatively scarce compared to available electron damage data. Also, the mechanisms are not well understood. It has been found most convenient to refer proton damage to an equivalent of 1 MeV electrons and then proceed to use the available data for electron damage. A curve for 1 ohm-cm and 10 ohm-cm N/P solar cells plotting the equivalent 1 MeV electron damage rate as a function of proton energy is shown in Fig. 3-6. The most important feature of this curve is the reciprocal dependence of damage upon proton energy for energies greater than 1 MeV. The curve has been drawn from available data, which definitely indicates a change in slope between 40 and 100 MeV. There appears to be a change in defect production mechanism in this range causing the change in slope.

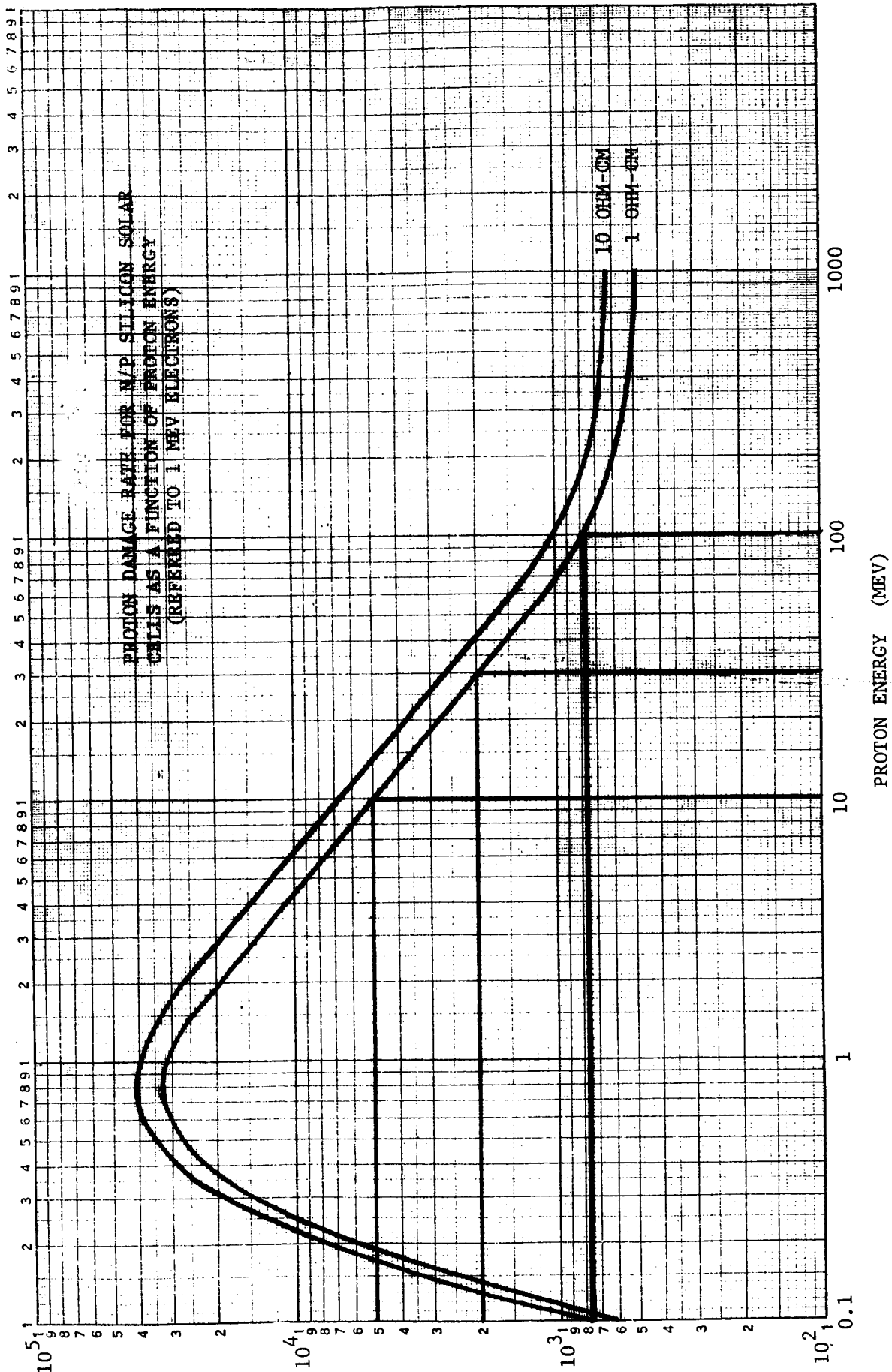


Figure 3-6.

In use, the proton flux is analyzed as a function of proton energy, and the equivalents for each energy are taken. The degradation may be found by referring to the electron damage curves for the flux obtained from the product of the proton flux and the damage equivalents.

The following curves, Figs. 3-6, 3-7, 3-8, and 3-9, used to represent the radiation damage effects, were taken from the space power manual, published by Hoffman Electronics Corporation.

Referring to Fig. 3-6, the following values of 1 MeV electron requirements are obtained for the flux/year data from JPL Document SE-003BB01-1-1B28.

	<u>Proton Flux</u>	<u>(Eq 1 MeV E/P)</u>	<u>1 MeV E Flux</u>
> 10	$1.6 \times 10^8$	$(5 \times 10^3)$	$8.0 \times 10^{11}$
> 30	$1.3 \times 10^8$	$(2 \times 10^3)$	$2.6 \times 10^{11}$
> 100	$9.3 \times 10^7$	$(7.6 \times 10^2)$	$7.1 \times 10^{10}$

Reference to the curves, Figs. 3-7, 3-8, and 3-9, for degradation of short circuit current, maximum power point, and open circuit voltage indicates that no degradation should be expected for a bare unprotected solar cell at the radiation anticipated.

The complete covering of the solar panel by the Tedlar film will form a protective barrier against low energy protons, in the range from 0.1 to 1.0 MeV. Low energy protons can cause solar cell degradation if they are allowed to impinge on the bare cell.

Cells filtered in the normal manner, with glass or quartz coverslips, usually have exposed active area due to the tolerances of the cell and filter. These bare areas can result in excessive power degradations. However, these bare areas are eliminated by using the proposed Tedlar film protective covering.

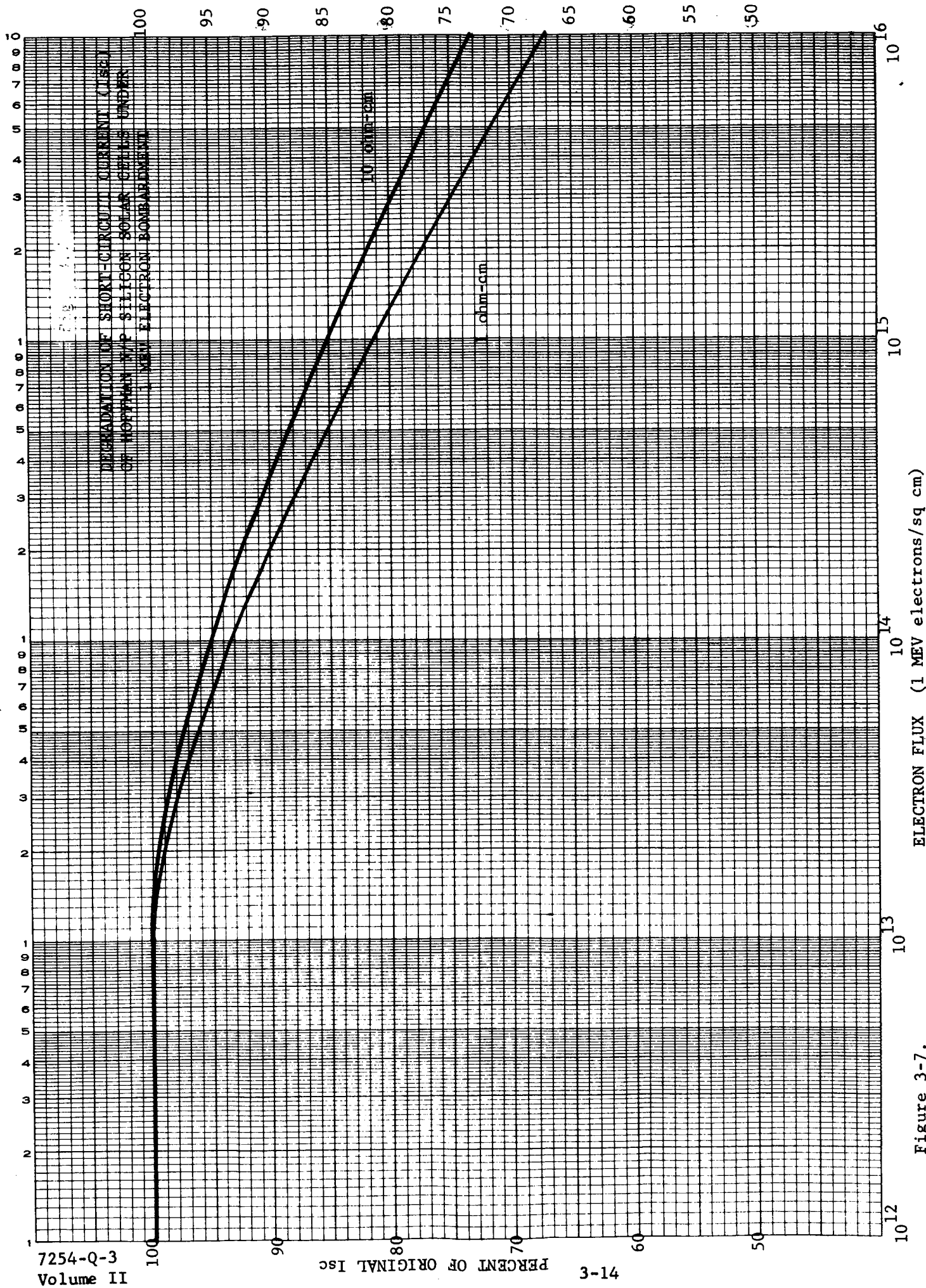


Figure 3-7.

15TR GRAPH SEMI-LOGARITHMIC  
4 CYCLES X 10 DIVISIONS PER INCH

SIGRA  
MADE IN U.S.A.

Y

Volume II 7254-Q-3

PERCENT OF ORIGINAL Pmax

3-15

Fig. 3-8  
DEGRADATION OF MAXIMUM POWER Pmax  
OF HORTON N/P SILICON SOLAR CELLS  
UNDER 1 MEV ELECTRON BOMBARDMENT

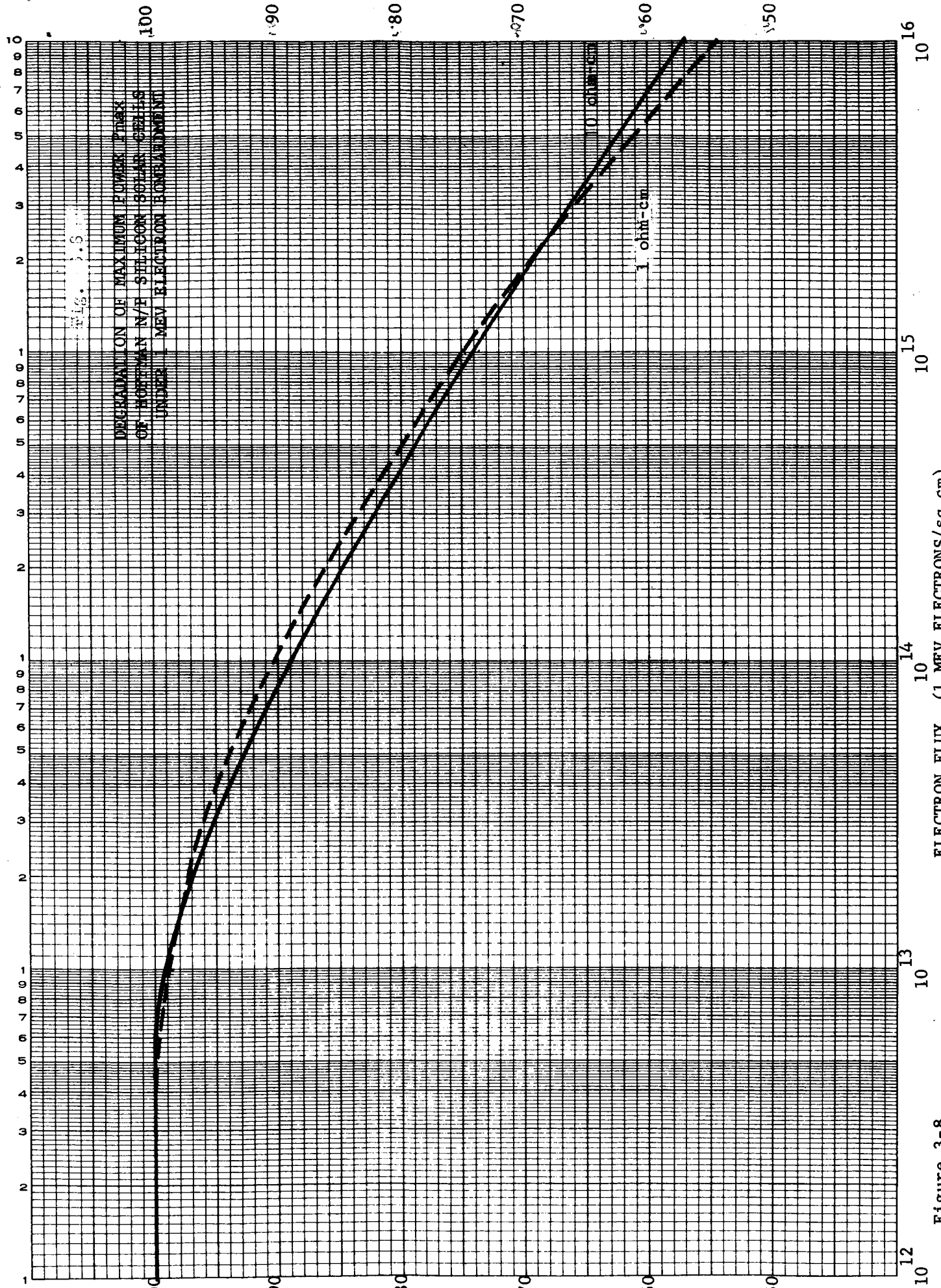


Figure 3-8

ELECTRON FLUX (1 MEV ELECTRONS/sq cm)

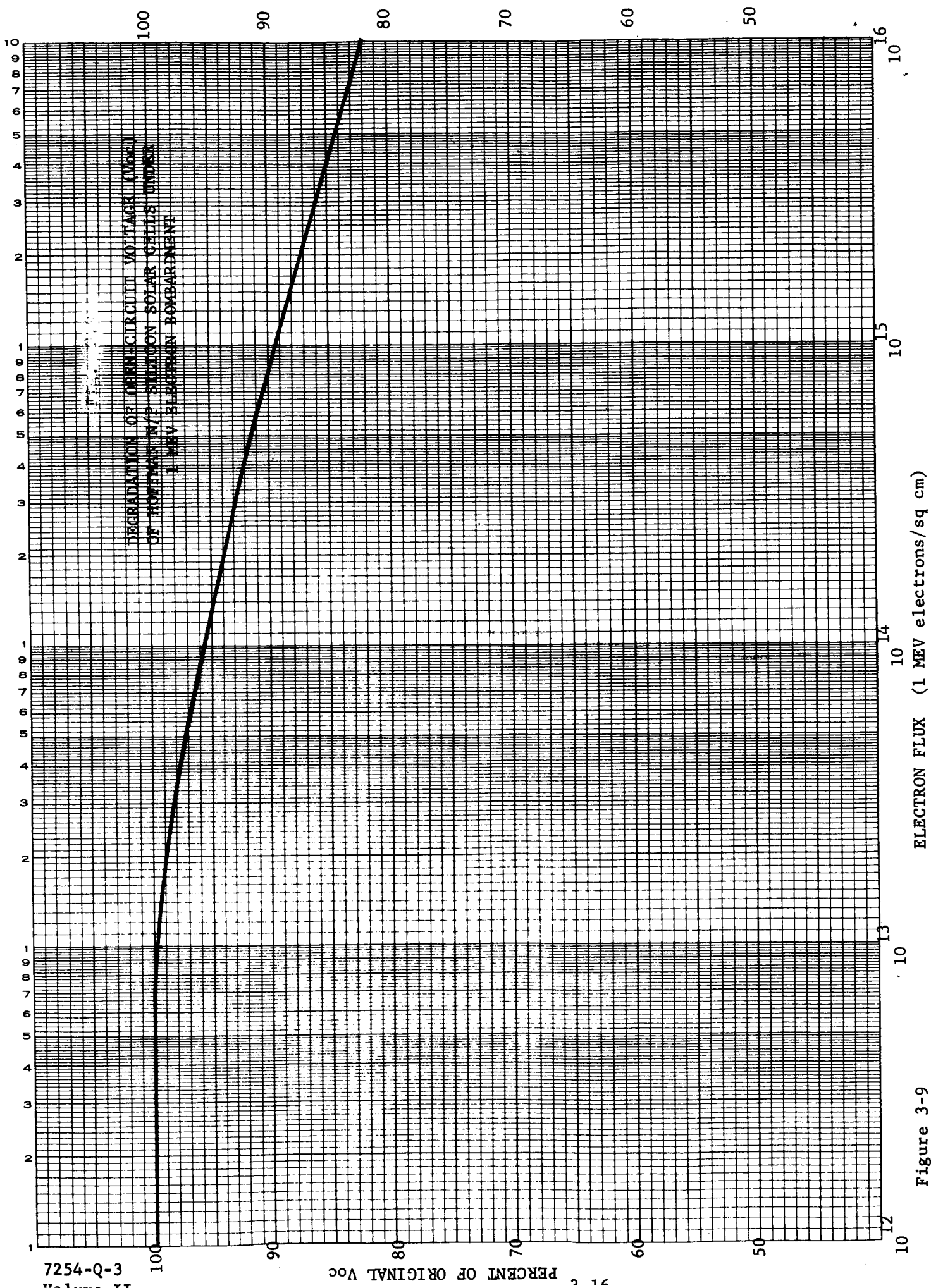


Figure 3-9

### 3.4 CIRCUIT DESIGN

The electrical circuit shall be a flat mounted array of series-parallel solar cells of 6P x 60S. The dimensions of the circuit are shown in Fig. 3-10. The electrical connector configurations are shown in Figs. 3-11 and 3-12. The reasons for preferring this type of circuit configuration were discussed in the 2nd quarterly report.

A drawing of a panel is shown in EOS Drawing No. 7254-118 Fig. 3-13. Each panel contains 20 solar cell circuits of 6P x 60S, and the circuits are alternated in direction to minimize the magnetic field effect. Each circuit is wired to a terminal board on the back side of the panel with two stranded wire leads for redundancy. Two isolation diodes are placed on the positive terminal board for each circuit, in series with the output leads. The circuits are wired in parallel with twisted stranded wire to an outlet plug on each panel.

### 3.5 ELECTRICAL POWER ANALYSIS

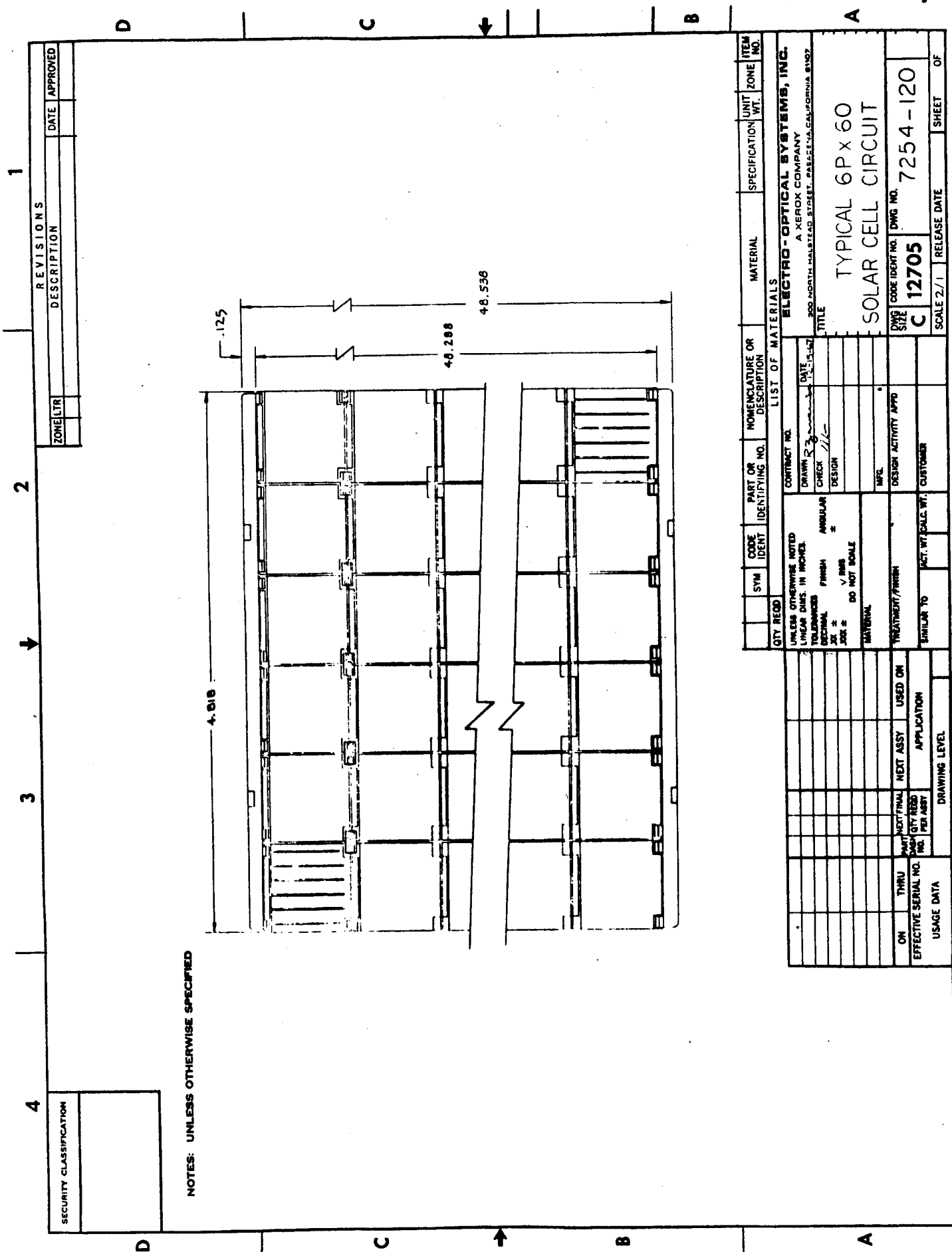
The preferred circuit was detailed in the 2nd Quarterly Report as being 6P x 66S. A closer look at the I-V characteristics of a 1-3 ohm-cm cell revealed that the operating point could be taken as 0.485V instead of 0.450V as originally assumed. An estimate of the temperature of the oriented array for noon sun conditions revealed that the average array temperature would be 28°C, near ambient.

A typical I-V curve of a cell at 28°C is shown in Fig. 3-2.

A new string length of 60 cells in series was selected. The operating point of the cell would be 28.0V plus 1 volt for diode and wiring losses:

$$29.0V/60 = 483 \text{ mV/cell}$$





NOTES: UNLESS OTHERWISE SPECIFIED

SECURITY CLASSIFICATION		REVISIONS		DATE		APPROVED	
ZONE/LTR		DESCRIPTION		DATE		APPROVED	
SYN		CODE	PART OR IDENTIFYING NO.	NOMENCLATURE OR DESCRIPTION	MATERIAL	SPECIFICATION	UNIT ZONE NO.
QTY REQD		UNLESS OTHERWISE NOTED	CONTRACT NO.	DATE	ELECTRO-OPTICAL SYSTEMS, INC.		
TOLERANCES		LINEAR DIMS. IN INCHES	DRAWN BY	11/11/66	A XEROX COMPANY		
DECIMAL		FINISH	CHECK	11/11/66	300 NORTH HALSTEAD STREET, PASADENA, CALIFORNIA 91367		
XX		ANGULAR	DESIGN	11/11/66	TITLE		
DO NOT SCALE		DO NOT SCALE	DATE	11/11/66	TYPICAL 6P x 60		
MATERIAL		DO NOT SCALE	DESIGN	11/11/66	SOLAR CELL CIRCUIT		
TREATMENT/FINISH		DO NOT SCALE	DATE	11/11/66	DWG NO. 7254-120		
SIMILAR TO		DO NOT SCALE	DESIGN ACTIVITY APPD	11/11/66	CODE IDENT NO. 12705		
ACT. WT. SCALE WT.		DO NOT SCALE	CUSTOMER	11/11/66	SCALE 2/1		
DRAWING LEVEL		DO NOT SCALE	RELEASE DATE	11/11/66	SHEET 1 OF 1		
ON THRU		DO NOT SCALE	USED ON	11/11/66	APPLICATION		
EFFECTIVE SERIAL NO.		DO NOT SCALE	APPLICATION	11/11/66	DRAWING LEVEL		
USAGE DATA		DO NOT SCALE	APPLICATION	11/11/66	DRAWING LEVEL		

Figure 3-10. Typical 6P x 60 Solar Cell Circuit



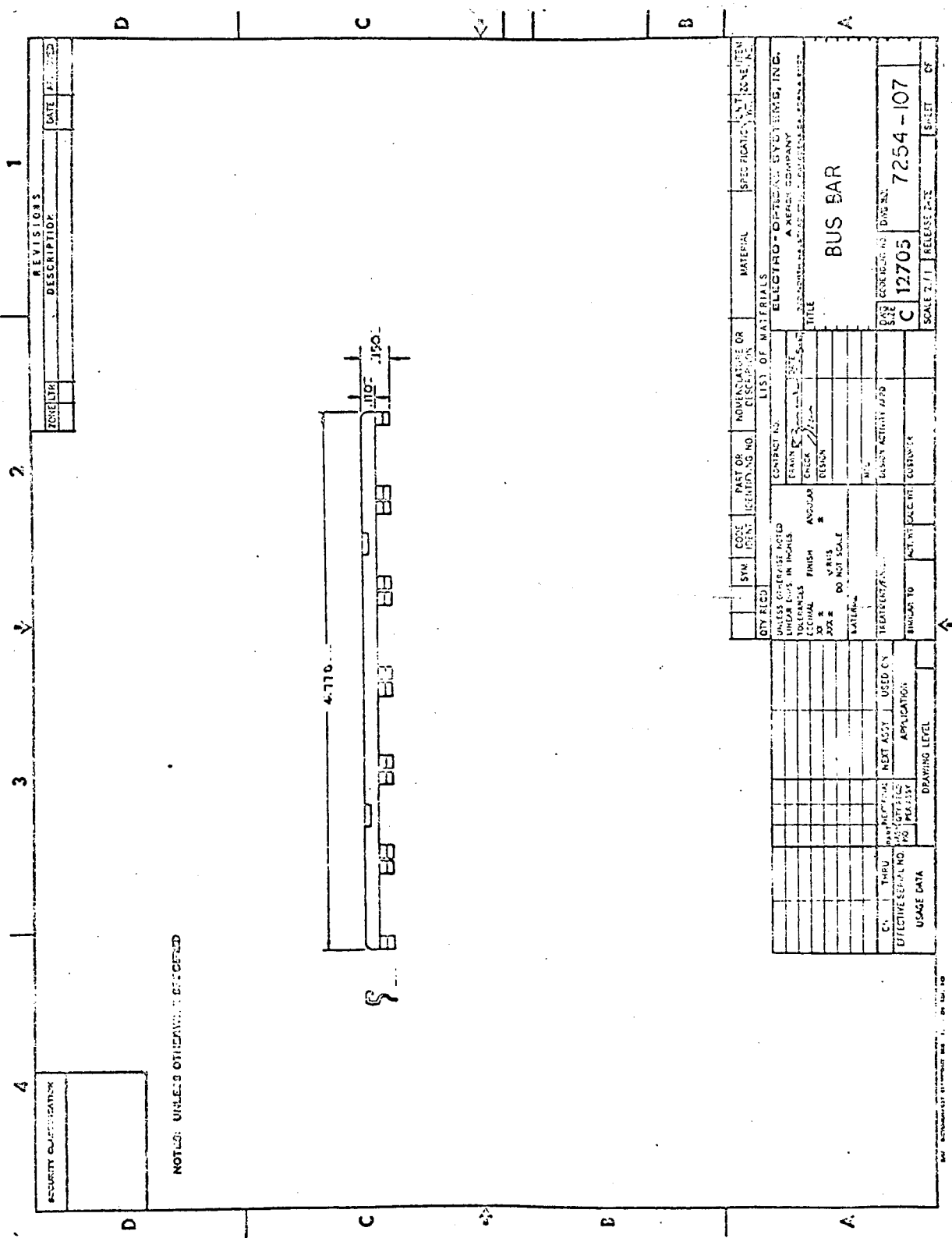
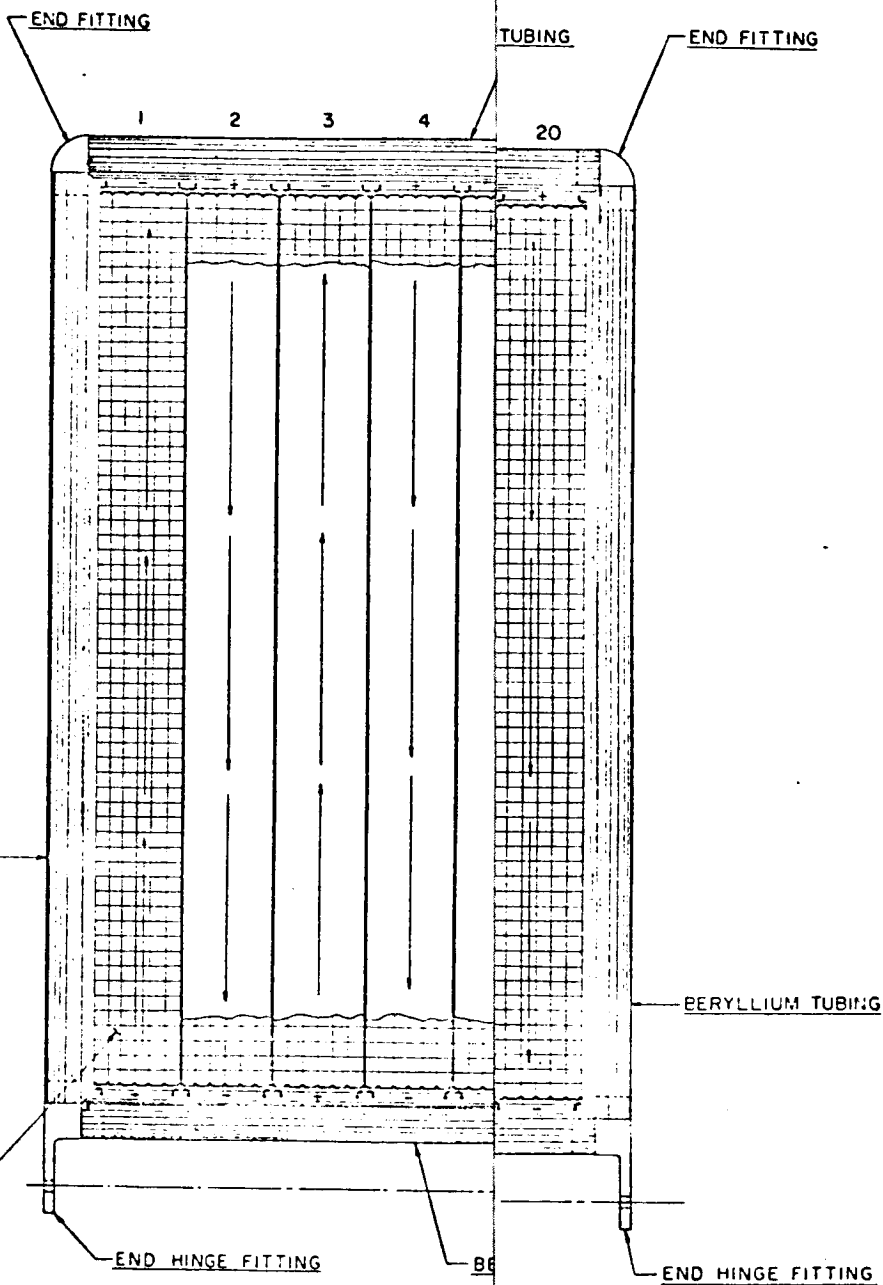


Figure 3-12. Bus Bar

NOTES: UNLESS

REVISIONS			
ZONE	LTR	DESCRIPTION	DATE APPROVED



CELL CIRCUIT  
S WIDE BY 60 CELLS LONG  
CUTS PER PANEL

7254-Q-3  
Volume I

NOVEMBER 1964	MATERIAL	SPECIFICATION	UNIT	ZONE	ITEM
NOV 1964					
LIST OF MATERIALS					
ELECTRO-OPTICAL SYSTEMS, INC.					
A HERRICK COMPANY					
100 WILSON BLVD. SUITE 100, BOSTON, MASSACHUSETTS 02118					
TITLE					
SOLAR PANEL ASSEMBLY					
HORIZONTAL BOOM DESIGN					
PLANETARY ARRAY					
DATE	DESIGNER	DATE	SCALE	DATE	SHEET
NOV 1964	J 12705	NOV 1964	7254 118	1	1

OUT FRAME

As discussed in the 2nd Quarterly Report, the shift in voltage due to the intensity change from  $140 \text{ mW/cm}^2$  to  $50 \text{ mW/cm}^2$  is 8 mV, ref. Fig. 3-14. Therefore, referring to Fig. 3-12, of a typical cell at  $28^\circ\text{C}$  the current output at 483 mV plus 8 mV (the 8 mV is added instead of subtracted to simulate shifting the curve) is 491 mV, which represents a current of 119.2 mA.

The submodule output would be:

$$6 (119.2 \text{ mA}) = 715.2 \text{ mA at } 483 \text{ mV}$$

The submodule output corrected for the Tedlar film coating and fabrication allowance:

Tedlar film coating	- 1%
Fabrication allowance	- 2%
Total	- 3%

Submodule output:

$$715.2 (0.97) = 694 \text{ mA at } 483 \text{ mV}$$

Circuit output = 694 mA at 28.0V  
(at 1 AU,  $28^\circ\text{C}$ )

The martian mission has been established as 1 earth year, approximately equivalent to the time period from martian spring through fall, as defined by the northern hemisphere. Figure 3-15 shows the seasonal position of Mars, and Figs. 3-16 and 3-17 show the inclination of Mars with respect to the Sun.

The attenuation of the Mars atmosphere was assumed to be a logarithmic function of pressure. By analogy with earth conditions, we assigned

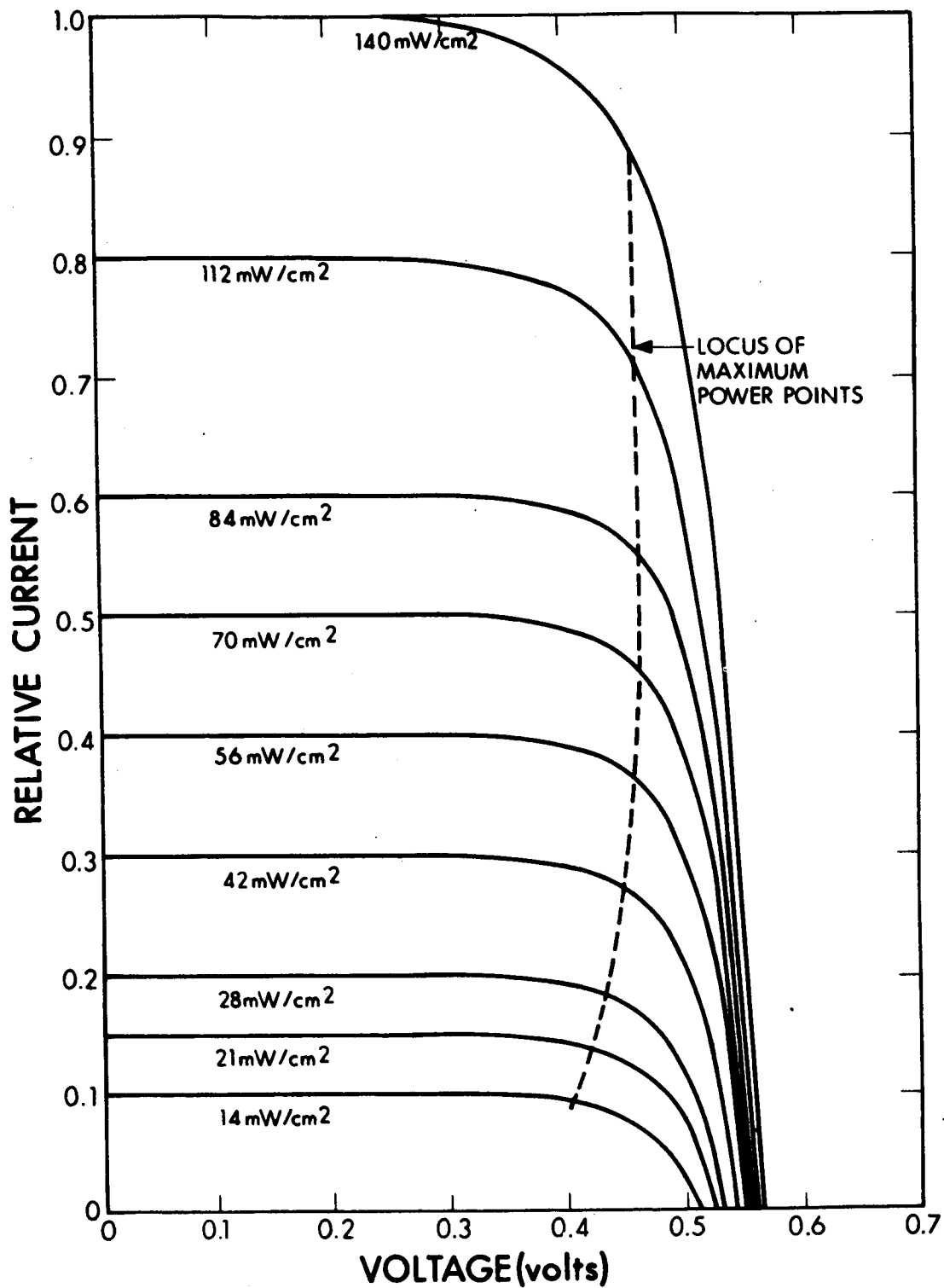


Figure 3-14. Typical I-V Characteristics as a Function of Solar Irradiation at Constant Temperature

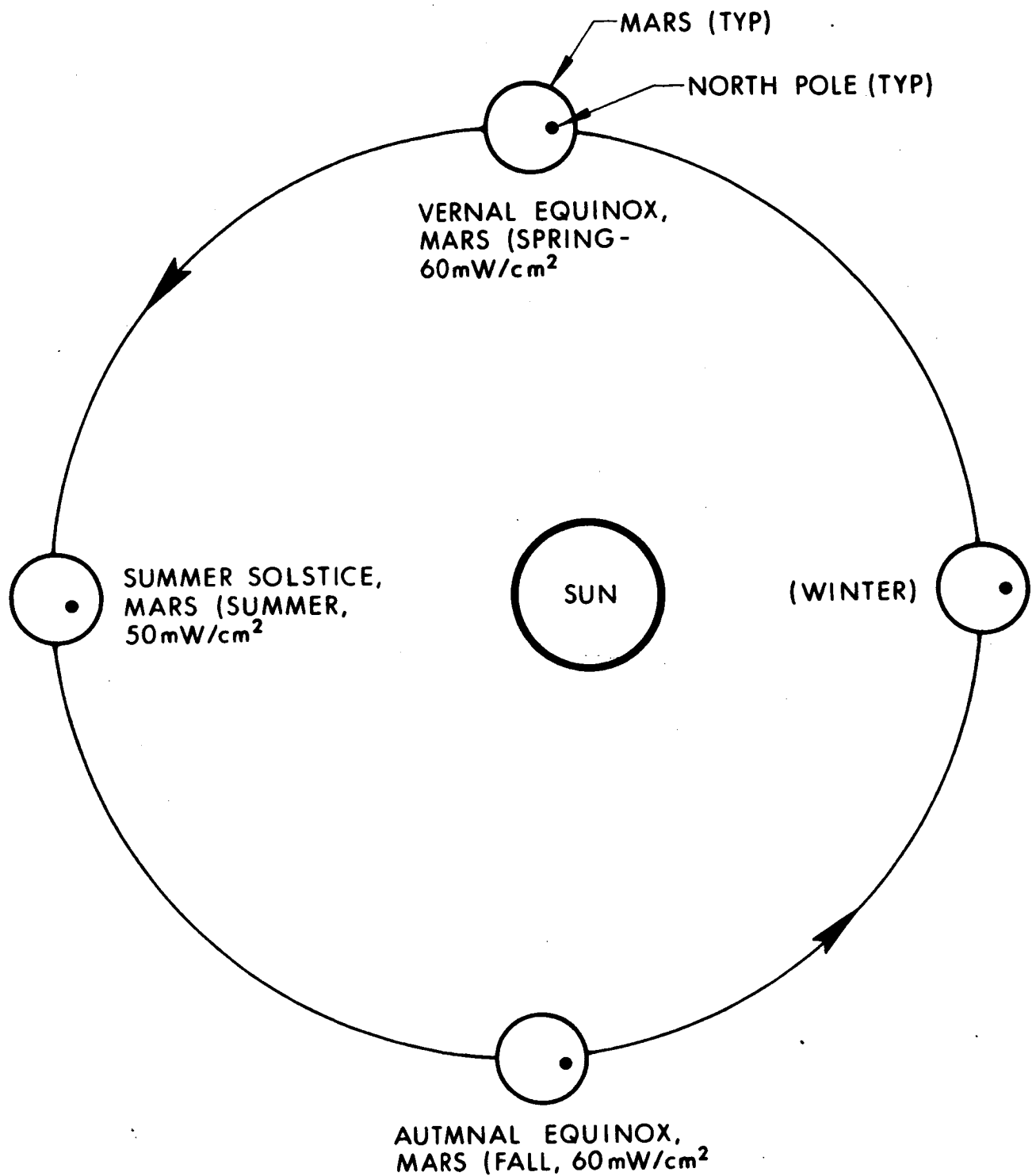


Figure 3-15. Positions of Mars During 1 Earth Year of Planetary Array Operation

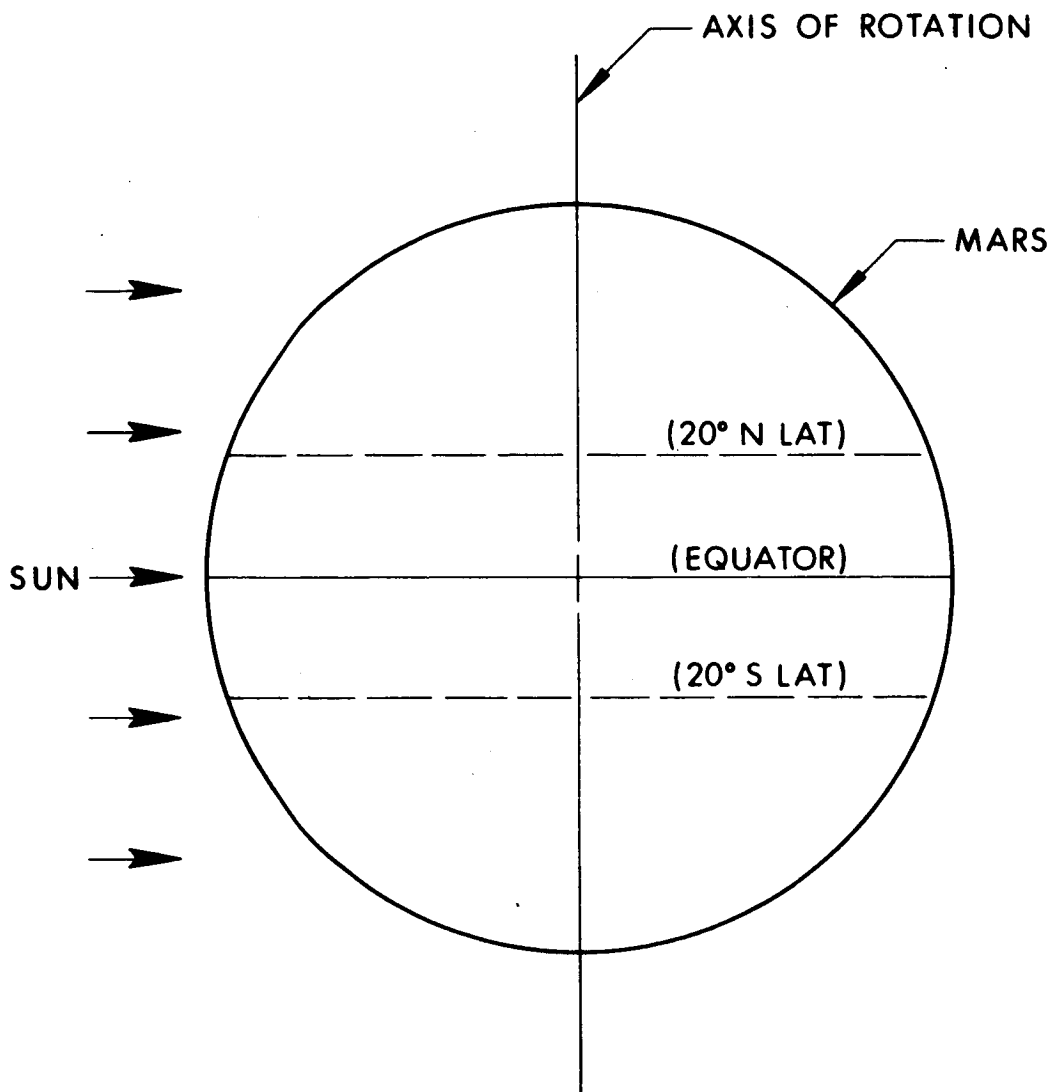


Figure 3-16. Position of Mars with Respect to the Sun at Noon for Spring and Fall



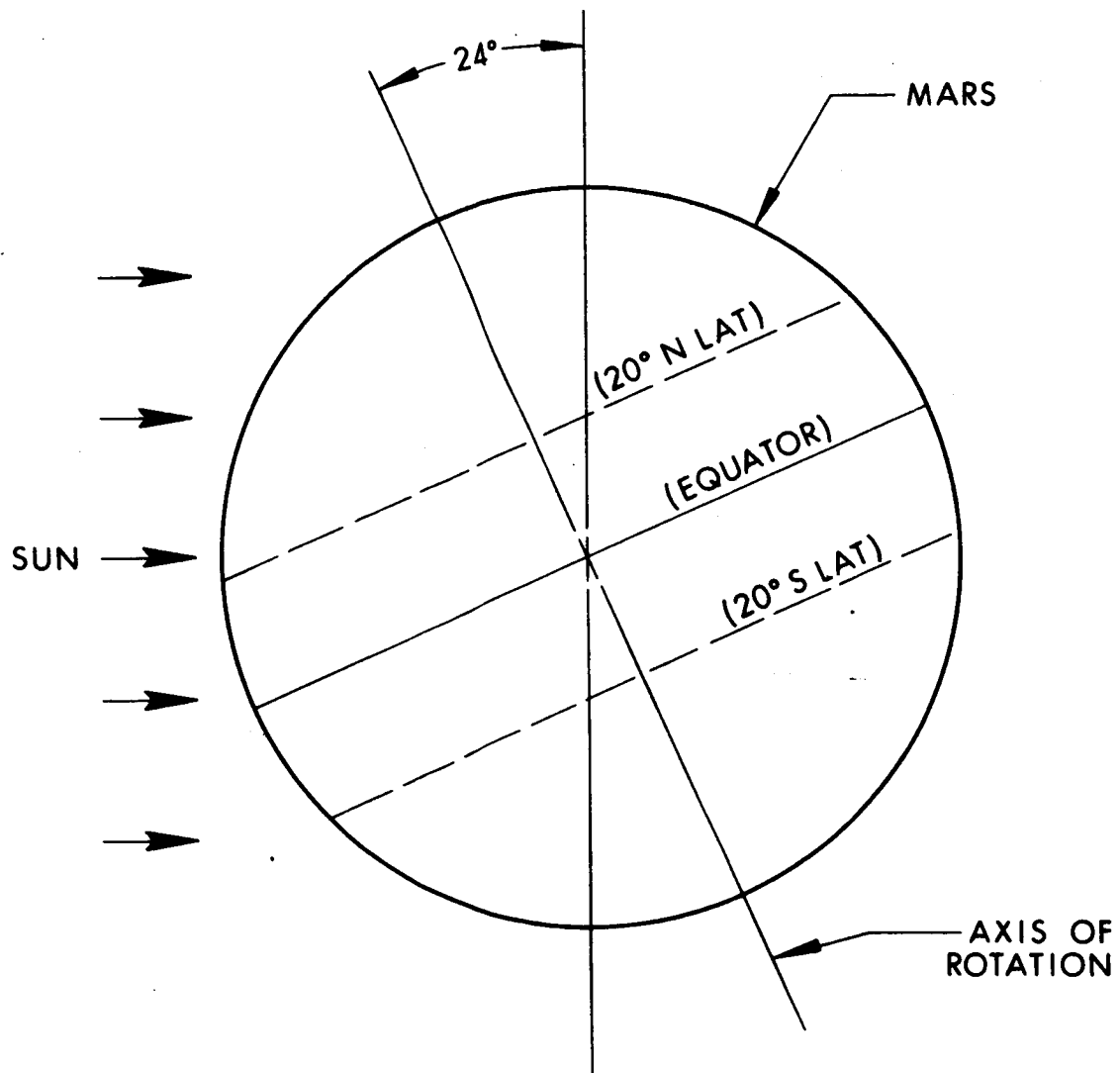


Figure 3-17. Position of Mars with Respect to the Sun  
at Noon for Summer

a transmission factor of 0.7 at a pressure of 1000 mb (earth AMI). The transmission factor at 1 mb was assumed at 1.0. By logarithmic extrapolation, the transmission factor at Mars surface (7 mb) was found to be 0.92. Reference Fig. 3-18 and the first Quarterly Report, para 2.1.4. We believe this transmission factor to be conservative; however, it has been established as a baseline for the program.

The Mars surface solar intensities are:

spring and fall;  
 $(60 \text{ mW/cm}^2) (0.92) = 55.2 \text{ mW/cm}^2$   
 Ratio to AMO =  $55.2/140 = 0.394$

summer;  
 $(50 \text{ mW/cm}^2) (0.92) = 46.0 \text{ mW/cm}^2$   
 Ratio to AMO =  $46.0/140 = 0.329$

Current output per circuit at Mars AMI,  $28^\circ\text{C}$  normal to the sun:

spring and fall;  
 $(694 \text{ mA}) (0.394) = 273.4 \text{ mA}$

summer;  
 $(694 \text{ mA}) (0.329) = 228.3 \text{ mA}$

Power output:

spring and fall;  
 $273.4 \text{ mA at } 28.0\text{V} = 7.66\text{W}$

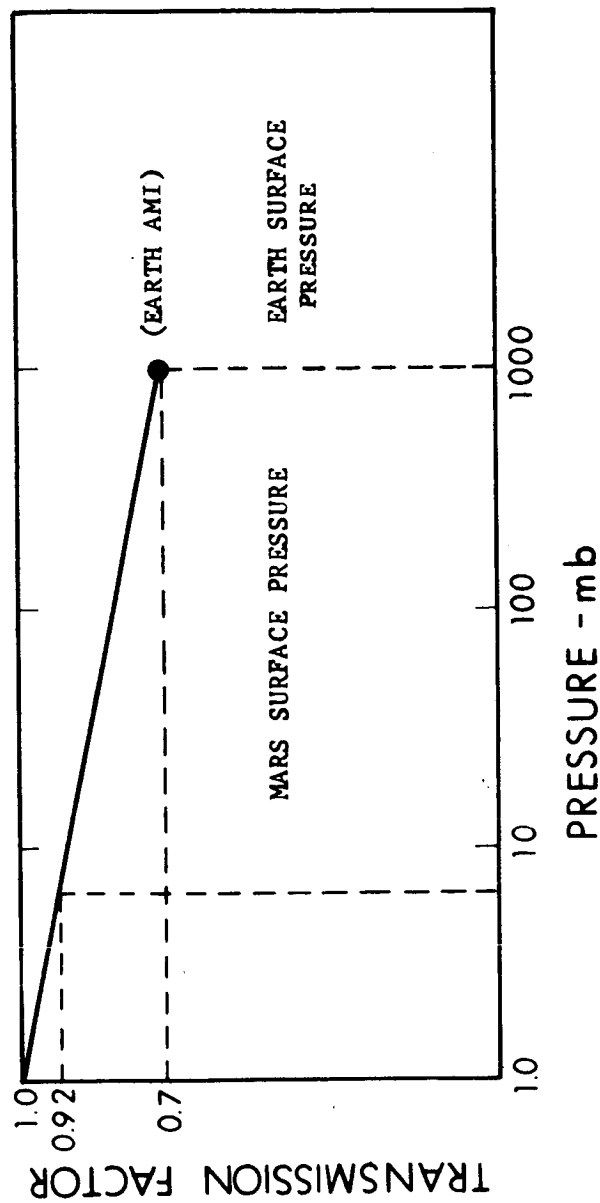
summer;  
 $228.3 \text{ mA at } 28.0\text{V} = 6.39\text{W}$

• NEAR MARS SPACE: 50 TO 74  $\text{mW/cm}^2$

• AT MARS SURFACE:

RECOMMENDED TRANSMISSION FACTOR AT AIR MASS ONE = 0.92

• RATIONALE:



• JUSTIFICATION:

- a) ONLY GAS MOLECULE SCATTERING CAN BE COMPUTED
- b) WATER VAPOR SCATTERING - UNKNOWN
- c) DUST SCATTERING - UNKNOWN
- d) WATER VAPOR ABSORPTION - UNKNOWN
- e)  $\text{CO}_2$  ABSORPTION CAN BE CALCULATED, BUT IT MAY BE NEGLECTED AS IT OCCURS AT LONG WAVELENGTHS (  $> 2.5 \mu$  )

Figure 3-18. Mars Solar Intensity

The actual power output of the two panel oriented array is a function of a number of variables; these are:

- a. Martian seasonal change in solar intensity, as a function of Mars-Sun distance.
- b. Number of circuits operational as a function of the masking effect of the antenna shadow, varying the number of circuits from a minimum of 30 to a maximum of 40.
- c. Temperature of the solar array, as a function of season latitude, and time of day.

It is not the intent of this report to analyze all the possible power output combinations. However, certain limiting conditions will be reviewed in detail, and it will be possible, by extrapolation, to estimate the power for any set of conditions.

The object of the two panel oriented solar array is to provide a three axis tracking capability, satisfying the packaging restraints imposed by JPL, without combining the antenna with the solar array. The deployment of the solar panels at the ends of a common boom eliminates the possibility of shadowing from the spacecraft body. The panels will see the shadow from the 48 inch diameter antenna, which, when the earth and sun are in line and with the spacecraft boom normal to the sun, will shade 10 circuits. This will be the maximum shading condition, for with the spacecraft in the same position, but the earth at  $90^\circ$  from the sun, the angle of the antenna will be approximately  $45^\circ$  and the shadow will be the  $\cos 45^\circ$  (0.707) (48). This is equal to 33.9 inches, and will shade 7 circuits at noon.

The temperature of the array affects the power output, and will vary during the day for any given location and season. A detailed thermal analysis is presented in Section 5; however the following average limiting conditions are cited for reference:

a. Oriented solar panel average temperatures.

1. First day of spring or fall,

Dawn -  $10.1^{\circ}\text{C}$

Noon -  $24.6^{\circ}\text{C}$

Sunset -  $20.5^{\circ}\text{C}$

2. First day of summer,

Dawn -  $0.2^{\circ}\text{C}$

Noon -  $15.3^{\circ}\text{C}$

Sunset -  $11.0^{\circ}\text{C}$

The power per circuit previously calculated for an estimated temperature at noon of  $28^{\circ}\text{C}$  can be corrected by the graph, Fig. 3-19. Therefore the power output of a circuit at summer noon, temperature  $15.3^{\circ}\text{C}$ , is as follows:

$$6.39 (1.073) = 6.856\text{W}$$

The minimum power output of the array at summer noon would be at the maximum shadow condition where only 30 circuits would be operating;

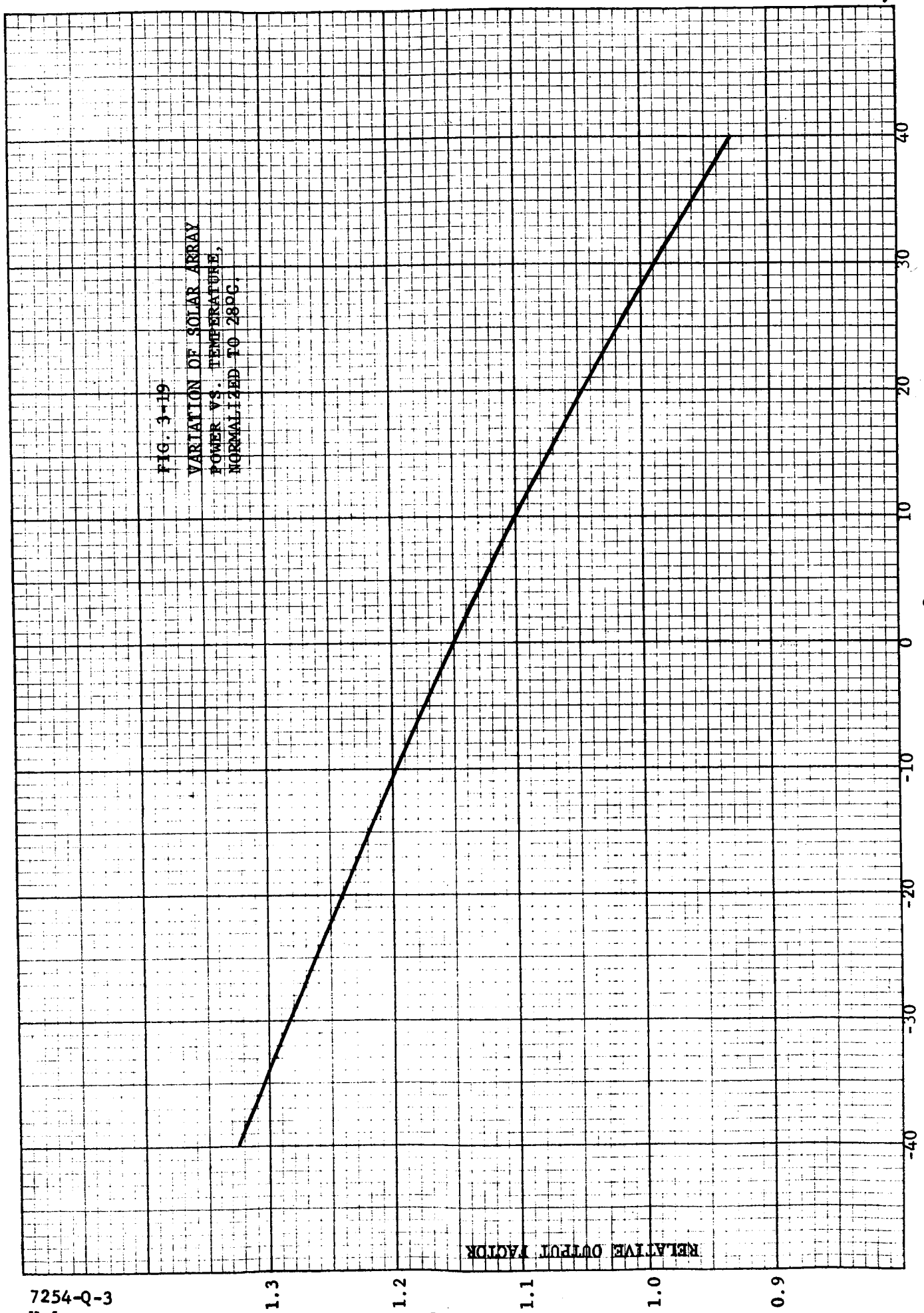
$$6.856\text{W} (30) = 205.7\text{W}$$

The correction for the array power at spring or fall noon to a temperature of  $24.6^{\circ}\text{C}$  would be:

$$7.66 (1.02) = 7.813\text{W}.$$

The power output of the array will vary dependent upon the number of circuits shadowed, the following is the power output of the array at noon for the limiting seasonal conditions:

FIG. 3-19  
VARIATION OF SOLAR ARRAY  
POWER VS. TEMPERATURE,  
NORMALIZED TO 28°C.



<u>No. Circuits</u>	<u>Summer</u>	<u>Spring/Fall</u>
30	205.7	234.2
31	212.5	242.2
32	219.4	250.0
33	226.2	257.8
34	233.1	265.6
35	239.9	273.5
36	246.8	281.3
37	253.7	289.1
38	260.5	296.9
39	267.4	304.7
40	274.2	312.5

It can readily be seen that the power output at noon exceeds the 200 watt minimum requirements.

The power output of the array fully oriented for a 12-hour daylight period (first day of summer) is affected by two variables. One is the change in temperature from sunrise to sunset; the other is the attenuating effects of the change in air mass for the same time period.

The temperature limits were given previously, and the air mass can be approximated for  $\pm 20^\circ$  latitude from the equator by equation:

$$A = [(R+H)^2 - R^2 \sin^2 \theta]^{1/2} - R \cos \theta$$

where

A = Air mass as a function of H

R = Radius of Mars (miles)

H = Atmosphere height of Mars (miles)

$\theta$  = Angle of rotation of Mars from solar noon ( $\pm 90^\circ$ )

The mean radius of Mars is fairly well established at 2100 miles; however, the atmosphere height of Mars is not known at the present. For the purposes of this report the atmospheric height of zero wind of 90,000 ft, taken from the wind predictions of estimated Voyager data furnished by JPL, will be doubled to give a maximum atmospheric height of 180,000 ft, or approximately 34 miles. Therefore, the ratio of  $R/H = 62$ . By substituting  $R = 62 H$  into the equation for A the following values are obtained:

<u><math>\theta</math> (time)</u>	<u>A</u>
0 (noon)	1.00
15° (1 hr)	1.04
30° (2 hr)	1.15
45° (3 hr)	1.42
60° (4 hr)	1.95
75° (5 hr)	3.52
90° (6 hr)	11.20

The effect of the air mass attenuation can be seen from the graph (Fig. 3-20-1) which is taken from the analysis presented in Fig. 3-18 of this report.

The panel power output for a 12-hour day (first day of summer) at the minimum seasonal solar intensity is plotted in Fig. 3-20-2. The solid line is the panel output corrected for temperature only, and the dashed line is the combined temperature and air mass corrected curve.

### 3.6 MAGNETIC FIELD ANALYSIS

An analysis was made to estimate the magnitude of the magnetic field created by the current carrying circuits of the solar array. The field resulting from the magnetization of materials is absent since all the array materials are nonmagnetic.



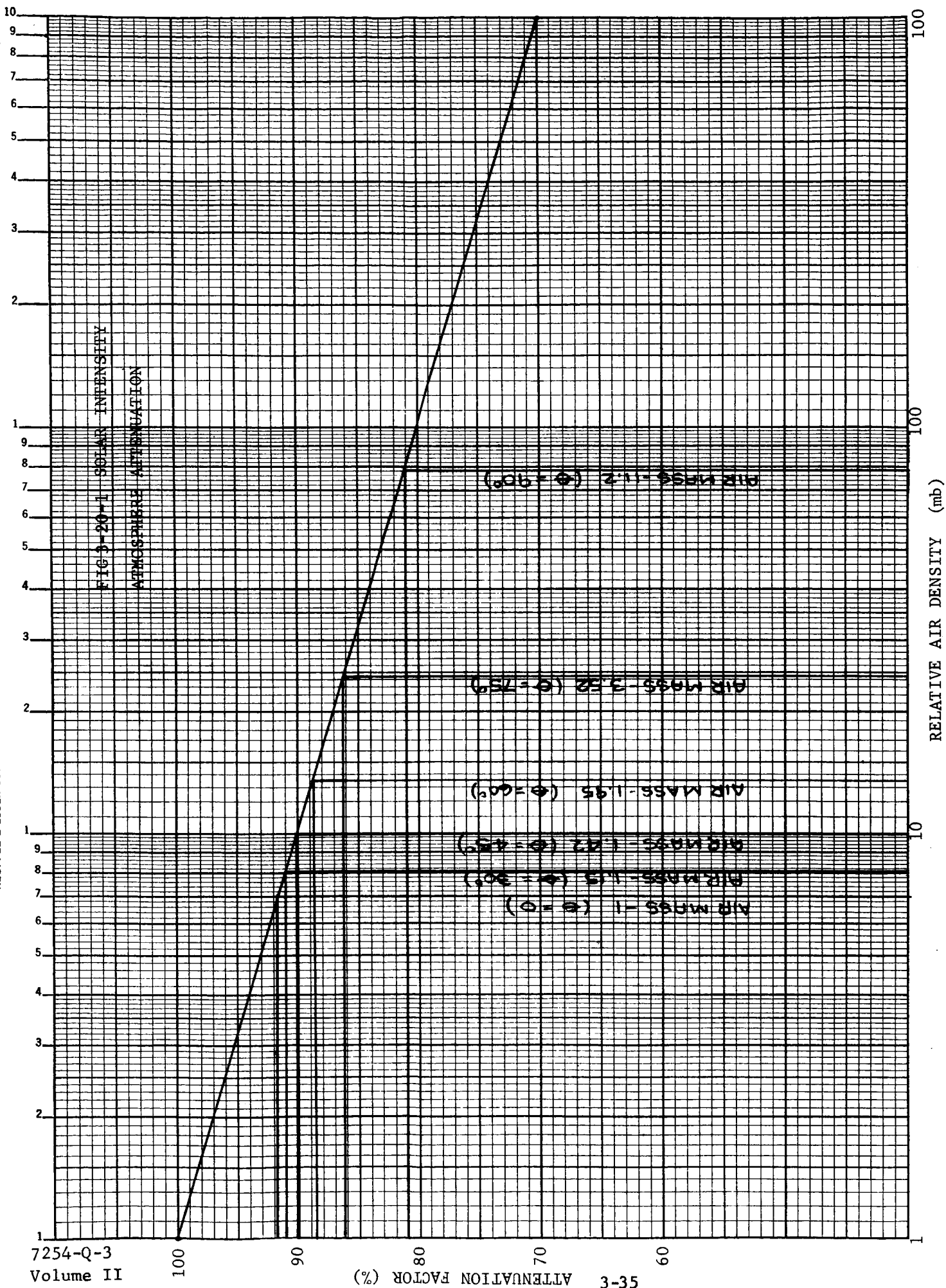
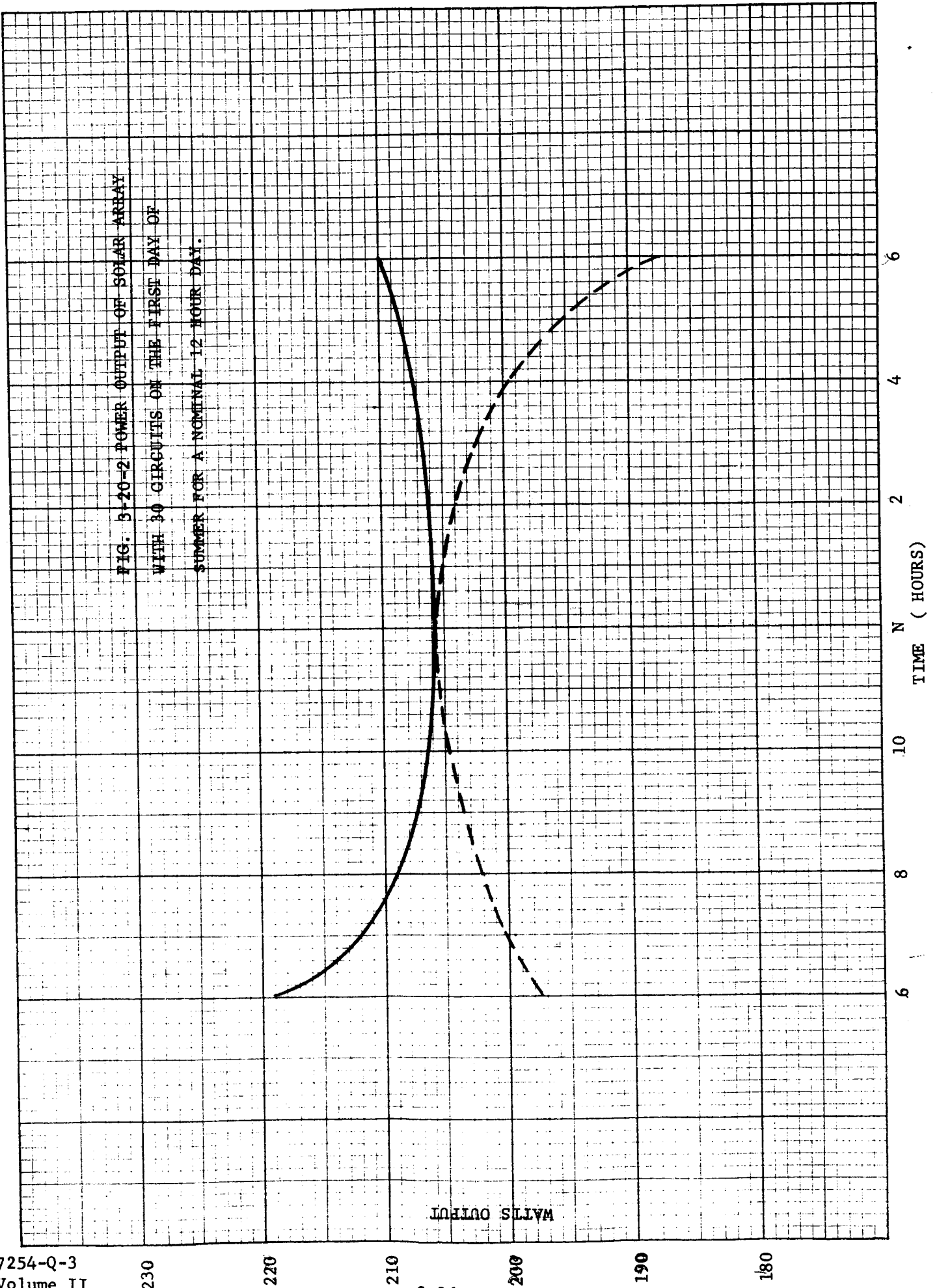


FIG. 3-20-2 POWER OUTPUT OF SOLAR ARRAY  
WITH 30 CIRCUITS ON THE FIRST DAY OF  
SUMMER FOR A NOMINAL 12 HOUR DAY.



The two panel oriented array has 20 circuits per panel, each circuit consisting of 6 cells in parallel by 60 cells in series. The maximum power per circuit occurs at noon conditions at spring and fall seasons of Mars, and at 28°C it is:

7.66W at 28.0V  
or, 0.274A at 28.0V

Each circuit is reversed in direction on the panel to form a minimum area current loop. The bus wire connections are made with twisted wire pairs to minimize the magnetic field effects. Figure 3-21 shows a typical circuit arrangement.

A calculation of the magnetic field can be effected by considering a pair of adjacent circuits as a current loop whose dipole moment is given by:

$$m = IA \quad (1)$$

where  $m$  is the dipole moment directed from the center of the loop and perpendicular to the plane of the loop;  $I$  is the circulating current; and  $A$  is the area of the loop in square meters. In the rationalized MKS units, the dipole moment is in amp-meter<sup>2</sup>.

The magnetic field due to the dipole at a point  $P$  can be divided into two components. Refer to Fig. 3-22.

$$B_r = \frac{\mu m}{2\pi r^3} (\cos\phi) \quad (2)$$

$$B_\phi = \frac{\mu m}{4\pi r^3} (\sin\phi) \quad (3)$$

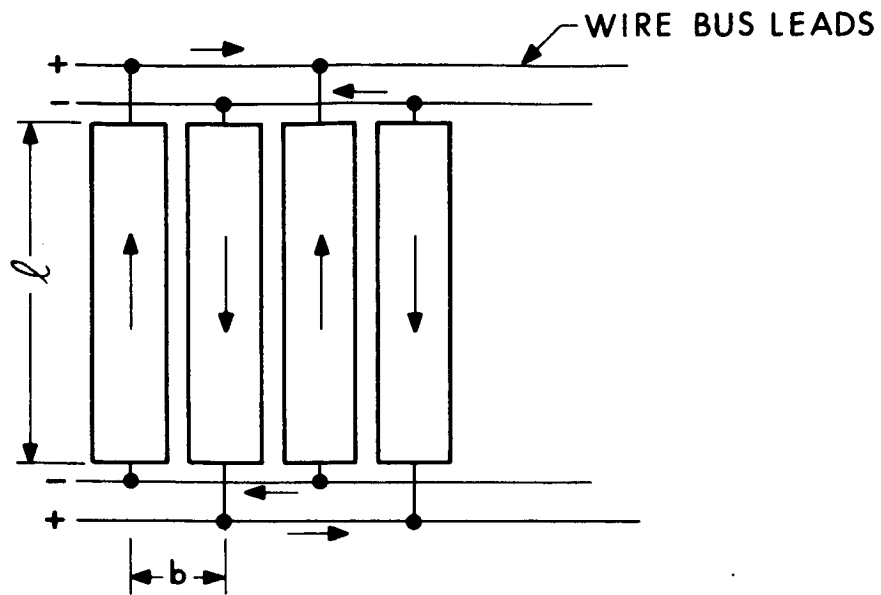


Figure 3-21. Bus and Circuit Arrangement

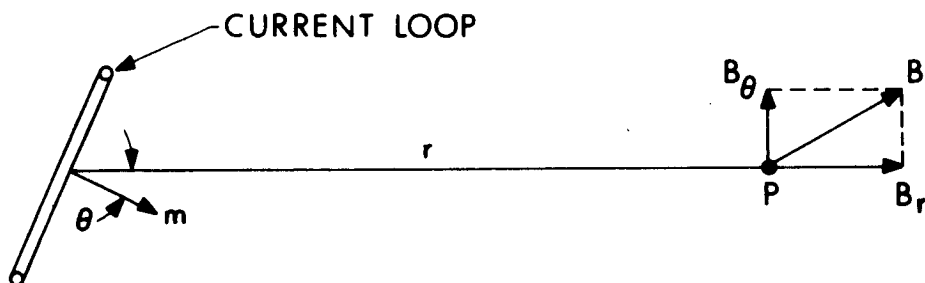


Figure 3-22. Coordinates of Dipole Field

Equations 2 and 3 are valid approximations when the characteristic dimension of the loop is small compared to the distance  $r$ .

The magnetic field at any point can be calculated by applying the three equations to the current loop formed by two adjacent circuits. The resultant field is the vector summation of the contribution of each individual loop. We shall assume that the instruments which are sensitive to the magnetic field are mounted in or near the spacecraft structure. Because the exact location of these instruments have not been specified we shall select a spot in the geometric center of the spacecraft with respect to the solar panels in order to illustrate the order of magnitude of the field.

#### 3.6.1 SUN AT THE ZENITH OF THE SPACECRAFT

For this case there is no shadowing and the current in all circuits is equal. It can be seen from Fig. 3-23 that the field will be zero by means of its symmetry. This is because, for a given dipole field, we can select another dipole which is directly opposite to cancel the field. At any other point adjacent to the spacecraft body the field will be not zero, but relatively weak and would not be worst case condition.

At any case where both panels are fully illuminated the field will be zero also. Refer to Fig. 3-24.

#### 3.6.2 SUN-SHADE CONDITION

When the shadow from the antenna partially shades the upper panel (Reference Fig. 3-25), an unbalanced condition is created with respect to the magnetic field cancellation. Due to the fact that the point P is out of plane with the center of the panel, the total unbalanced magnetic flux may be found by vector analysis of the field intensity

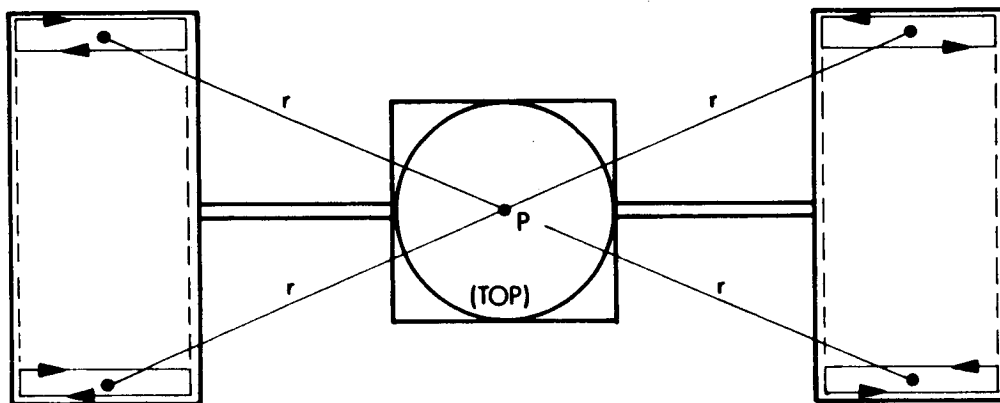


Figure 3-23. Geometric Relationship of Current Loops with Respect to the Spacecraft with Panels Parallel with Boom Arms

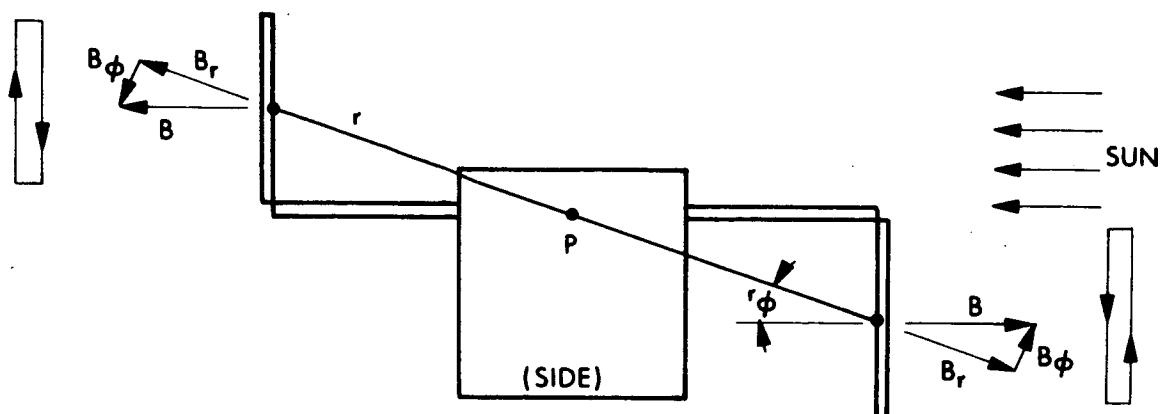


Figure 3-24. Geometric Relationship of Current Loops with Respect to the Spacecraft with the Panels Normal to the Boom Arm and Fully Illuminated

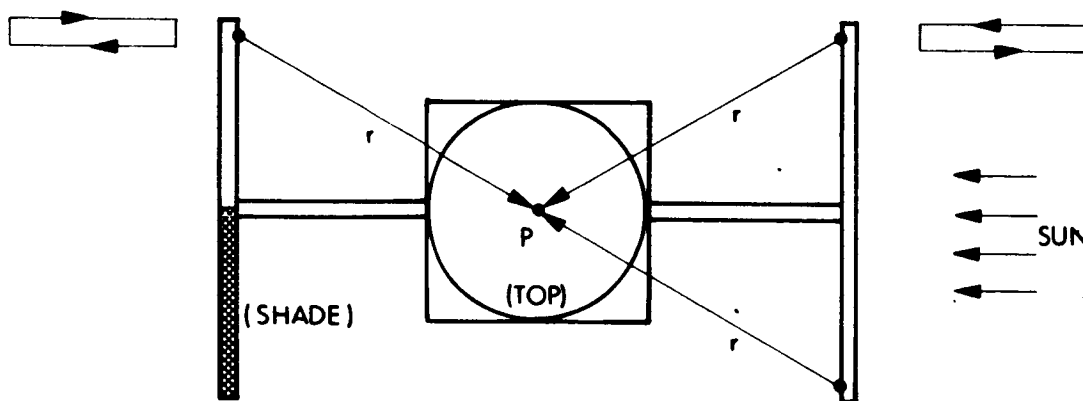


Figure 3-25. Geometric Relationship of Current Loops with Respect to the Spacecraft with the Panels Normal to the Boom Arms and Under Maximum Shade Conditions

in the X-Y and Y-Z planes. Refer to Fig. 3-26 (a) and (b). The following approximate values will be used.

$$\begin{aligned}\mu &= 4\pi \times 10^{-7} \text{ henries/meter} \\ I &= 0.274 \text{ amps} \\ A &= 0.122 \times 1.22 = 0.148 \text{ meter}^2 \\ \theta &= 17^\circ 30' \\ r_1 &= 100 \text{ inches (2.54 meters)} \\ r_2 &= 101 \text{ inches (2.55 meters)} \\ r_3 &= 103 \text{ inches (2.62 meters)} \\ r_4 &= 106 \text{ inches (2.70 meters)} \\ r_5 &= 110 \text{ inches (2.80 meters)} \\ \beta_1 &= 2^\circ 52' \\ \beta_2 &= 8^\circ 33' \\ \beta_3 &= 14^\circ 5' \\ \beta_4 &= 19^\circ 20' \\ \beta_5 &= 24^\circ 12'\end{aligned}$$

The results of the vectors in the (X-Y) plane are as follows:

$$\begin{aligned}B_{r_T} &= \frac{\mu m}{2\pi r_1^3} (\cos\beta_1) + \dots + \frac{\mu m}{2\pi r_5^3} (\cos\beta_5) \\ &= 0.081 \times 10^{-7} (0.061 + 0.059 + 0.054 + 0.048 + 0.041) \\ &= 2.13 \times 10^{-9} \text{ weber/meter}^2 \\ B_{\beta_T} &= \frac{\mu m}{4\pi r_1^3} (\sin\beta_1) + \dots + \frac{\mu m}{4\pi r_5^3} (\sin\beta_5) \\ &= 0.0405 \times 10^{-7} (0.0031 + 0.0089 + 0.0135 + 0.0169 + 0.0187) \\ &= 0.247 \times 10^{-9} \text{ weber/meter}^2\end{aligned}$$



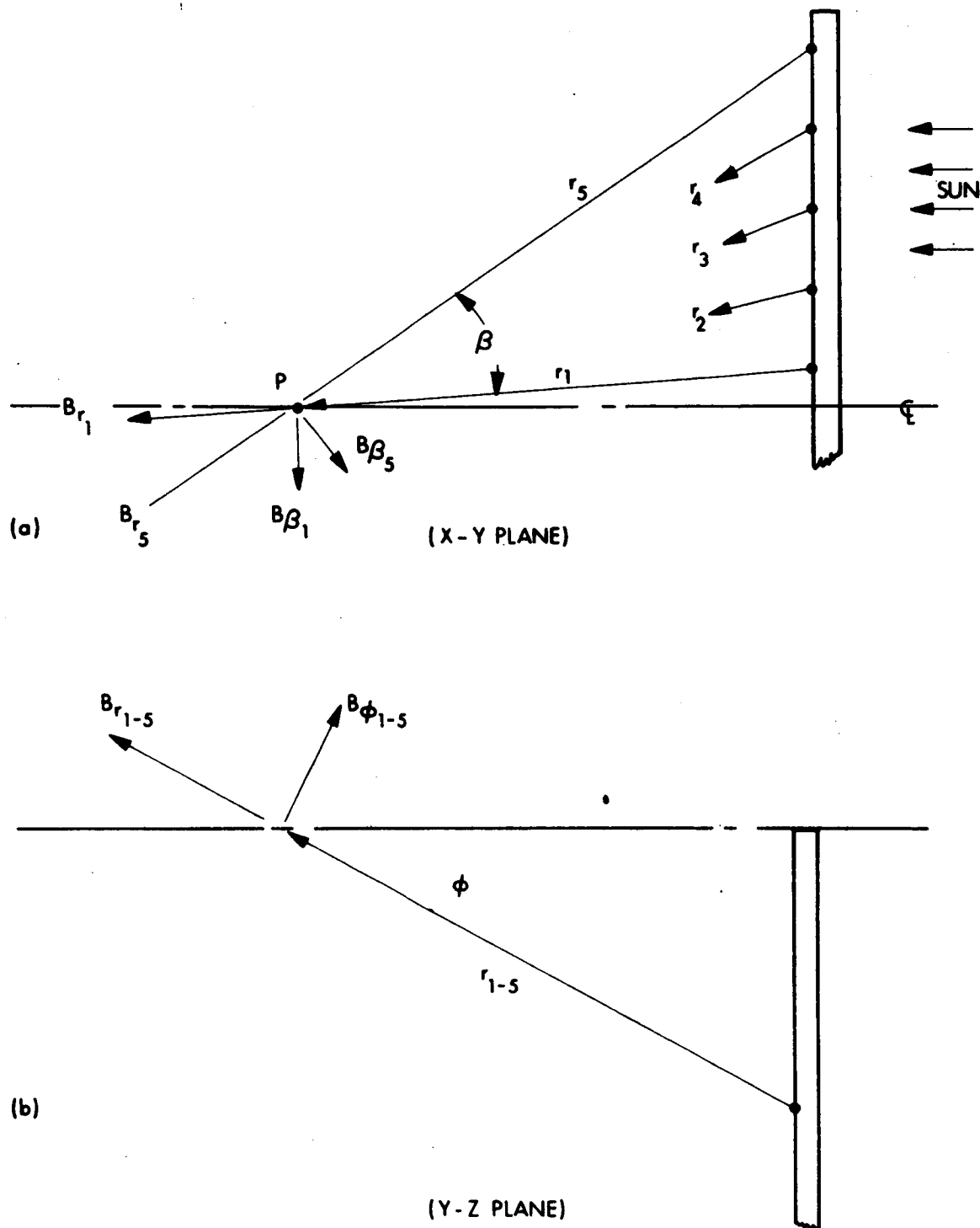


Figure 3-26. Field Vectors Due to Five Current Loops Uncanceled Due to Shadow on Opposite Panel

$$B_{(X-Y)} = (\beta_{r_T})^2 + (\beta_{B_T})^2$$

$$B_{(X-Y)} = 2.14 \times 10^{-9} \text{ weber/meter}^2$$

The results of the vectors in the (Y-Z) plane are as follows:

$$B_{r_T} = \frac{\mu m}{2\pi r_1^3} (\cos\phi) + \dots \frac{\mu m}{2\pi r_5^3} (\cos\phi)$$

$$= 0.081 \times 10^{-7} (0.0582 + 0.0575 + 0.0531 + 0.0485 + 0.0434)$$

$$= 2.12 \times 10^{-9} \text{ weber/meter}^2$$

$$B_{\phi_T} = \frac{\mu m}{4\pi r_1^3} (\sin\phi) + \dots \frac{\mu m}{4\pi r_5^3} (\sin\phi)$$

$$= 0.0405 \times 10^{-7} (0.0183 + 0.0181 + 0.0167 + 0.0153 + 0.0137)$$

$$= 0.332 \times 10^{-9} \text{ weber/meter}^2$$

$$B_{(Y-Z)} = \sqrt{(\beta_{r_T})^2 + (\beta_{\theta_T})^2}$$

$$= 2.14 \times 10^{-9} \text{ weber/meter}$$

The total flux at P is equal to the vector sum of  $B_{(X-Y)} + B_{(Y-Z)}$ :

$$B_T = \sqrt{(\beta_{(X-Y)})^2 + (\beta_{(Y-Z)})^2}$$

$$= 3.02 \times 10^{-9} \text{ weber/meter}^2$$

$$= 3.02 \text{ gamma}$$

### 3.6.3 CONCLUSION

The magnetic flux at point P is quite low as a result of the worst case shadowing. Placement of the instrument at some other location other than P would alter field intensity slightly, dependent upon location.

## SECTION 4

### STRUCTURAL DESIGN AND ANALYSIS

This section contains the following information:

- a. A functional description of each of the major mechanical components of the 2-axis solar array baseline configuration.
- b. A discussion of the criteria used to select the material for each component.
- c. A description of the mathematical model(s) used to analyze each component.
- d. The loads analysis performed to establish the critical loading condition for each component.
- e. The stress analysis for each component and a summary of the respective margins of safety.
- f. Conclusions and recommendations.

The mechanical components of the array are:

- a. Substrate
- b. Rotating boom
- c. Substrate support truss

#### 4.1 SUBSTRATE

##### 4.1.1 DESCRIPTION

There are two substrate panels required per spacecraft. Each substrate panel is approximately 104 inches by 54 inches, with an area of  $39.0 \text{ ft}^2$ . Each of these is made of two hollow core, framed subpanels which are segments of a sphere. The radius of the spherical surface is 155.5 inches. The planform of each subpanel is approximately 52 x 54 inches, with a nominal thickness of the panel section of 0.1 inch.

#### 4.1.2 MATERIAL SELECTION

The substrate material chosen for this configuration is electroformed aluminum hollow core. This material was chosen for this application based on the following considerations:

- a. Fabrication: The electroforming fabrication technique eliminates in-process handling of foil gage materials and difficult bonding operations required to produce comparable types of sandwich shell structures.
- b. Weight: The one-piece structure which results from the electroforming process is lighter than laid-up sandwich structures of equivalent stiffness.

#### 4.1.3 MATHEMATICAL MODELS

- a. Dynamic launch load: The model used to calculate the dynamic internal loads during launch assumes a substrate panel which is simply supported along its periphery. The external loads were assumed to act normal to the plane which is tangent to the substrate at its center.
- b. Wind loading: The substrate panels were assumed to be flat plates placed normal to the direction of the wind for worst case loading.

#### 4.1.4 CRITICAL LOAD ANALYSIS

- a. Launch load: The first fundamental resonant frequency of the substrate was determined by using the following equation:

$$f_n = \frac{1}{2\pi} \left[ \frac{g}{\rho h} \left( D \{ \lambda_1^2 + \mu_1^2 \}^2 + \frac{Eh}{R^2} \right) \right]^{1/2}$$

where:  $g = 386 \text{ IPS}^2$   
 $\rho h = (\text{hollow core and dead load wt/area}) = 1.31 \times 10^{-3} \text{ psi}$   
 $E = 7.8 \times 10^6 \text{ psi}$   
 $I = 1.58 \times 10^{-6} \text{ in}^4/\text{in}$

$$\begin{aligned}
D &= EI = 12.32 \text{ lb-in}^2/\text{in} \\
\lambda_1 &= \pi/\alpha = 5.817 \times 10^{-2}/\text{in} \quad \alpha = 54 \\
\mu_1 &= \pi/\beta = 6.041 \times 10^{-2}/\text{in} \quad \beta = 52 \\
R &= (\text{radius of curvature}) = 155.5 \text{ in} \\
h' &= (\text{effective height based on area}) \\
&= \left[ 2 + \left(\frac{h}{a}\right) - \frac{\sqrt{3}}{2} \left(\frac{d}{a}\right) \right] t
\end{aligned}$$

where  $h = 0.10 \text{ in}$

$a = 0.525 \text{ in}$

$d = 1.00 \text{ in}$

$t = 0.004 \text{ in}$

$\therefore h' = 2.165 \times 10^{-3} \text{ in}$

and

$$f_n = \frac{1}{2\pi} \left[ \frac{386}{1.31 \times 10^{-3}} \left( 12.32 \{5.817^2 + 6.041^2\} 10^{-8} + \frac{(7.8 \times 10^6)(2.1641 \times 10^{-3})}{1.555^2 \times 10^4} \right) \right]^{1/2}$$

$$f_n = 72.23$$

For an input load of 1.5 g at 72.2 Hz (see 7254-Q-1) the maximum deflection of the substrate occurs at its center and has a magnitude of 0.228 inch which was determined by the following equation:

(See 7027-1DR, 18 May 1966, Appendix E)

$$W = \frac{16}{\pi^2} \frac{Q}{(2\pi f_n)^2} \bar{W}(\alpha, \beta) \ddot{W}_s$$

where  $Q$  = dynamic magnification = 50

$$\bar{W} = 1 \text{ (at center of panel)}$$

$$W_s = \text{sinusoidal input at } 72 \text{ Hz} = 1.5g$$

$$\omega_{11} = 2\pi f_n = 453.834$$

$$\therefore W = \frac{16(50)(1)(1.5)(386)}{\pi^2 (453.834)^2}$$

$$\ddot{W} = 0.228 \text{ inch}$$

The maximum acceleration response at the center of the substrate to an input load of 1.5g is:

$$\ddot{W} = \frac{16}{\pi^2} Q \ddot{W}_s$$

$$\ddot{W} = \frac{16}{\pi^2} (50)(1.5)$$

$$\ddot{W} = 121.6g \text{ (0-peak)}$$

b. Wind Load: The total wind load on a flat plate is given by the relation:

$$F = 1/2 C_D \rho A V^2$$

where  $F$  = total force in lb

$C_D$  = a coefficient depending on aspect ration, a/b, and the angle between the plate and the wind flow,  $\alpha$

$A$  = total area of plate in  $\text{ft}^2$

$\rho$  = the mass density of the atmosphere (Mars)  $\text{lb-sec}^2/\text{ft}^4$

$V$  = wind velocity in ft/sec

The specific parameters for the concept being analyzed are:

$$a/b = 2$$

$$\alpha = 90^\circ \text{ worst case}$$

$$C_D = 1.16$$

$$A = 39.0 \text{ ft}^2$$

$$\rho = 3.59 \times 10^{-5} \text{ lb-sec}^2/\text{ft}^4$$

$$V = 325 \text{ ft/sec (free stream velocity} \times 0.67 + \text{gusts) i.e.,}$$

$$V = (186 \times 0.67 + 200)$$

$$F = 1/2 (1.16)(3.59) \times 10^{-5} (39.0) (325)^2$$

$$F = 85.77 \text{ lb}$$

The average pressure on the substrate due to the wind loading is 2.19 lb/ft<sup>2</sup> or 0.0152 psi. This average applied pressure is small compared to the equivalent average applied pressure of 0.159 psi which results from the random vibration loading. The design load for the substrate will be a pressure of 0.159 psi.

#### 4.1.5 STRESS ANALYSIS

The membrane force per unit length is determined by:

$$\frac{P}{l} = \frac{\rho R}{2}$$

where  $\frac{P}{l}$  = membrane force per unit length - lb/in

$R$  = radius of curvature = 155.5 in

$\rho$  = (applied pressure) =  $(\text{SpWt})_p \times g$

where  $\text{SpWt} = (\text{specific weight}) = 1.31 \times 10^{-3} \text{ psi}$

$g = \ddot{W} = 121.6 \text{ (o-peak) g}$

$\rho = 0.159 \text{ psi}$



## 4.2 STRUCTURE

### 4.2.1 ROTATING BOOM

The rotating boom is a torque tube which passes through the spacecraft body and synchronizes the movement of the two panels in one of the two axes of rotation. This tube is supported in bearings at the spacecraft body and at the ends of the boom. The bearing design at the ends of the boom is such that it takes up the bending moment resulting from the weight and wind loads exerted by the panels. The boom is loaded in torsion only.

The boom material will be a beryllium tube to take advantage of the high shear strength and low weight of the material. The dimensions of the tube are: length - 170 inches, diameter - 2.000 inches, and a wall thickness of 0.020 inch.

The maximum wind loading condition is assumed to be the stagnation pressure of  $2.19 \text{ lb/ft}^2$  applied to the opposite sides of the panel about the axis of rotation. This loading condition is somewhat improbable due to the balanced design of the panel; however, it can be approached by edge on wind loading especially under the buffeting wind gusts. Figure 4-1 describes the torsional wind loading condition. The resultant force per side, F, is:

$$F = \frac{2.19 \text{ lb/ft}^2 (19.5 \text{ ft}^2)}{2}$$
$$= 21.3 \text{ lb}$$

The moment about the axis of rotation is:

$$M = 21.3 \text{ lb} (34.6 \text{ in}) = 739 \text{ in-lb}$$

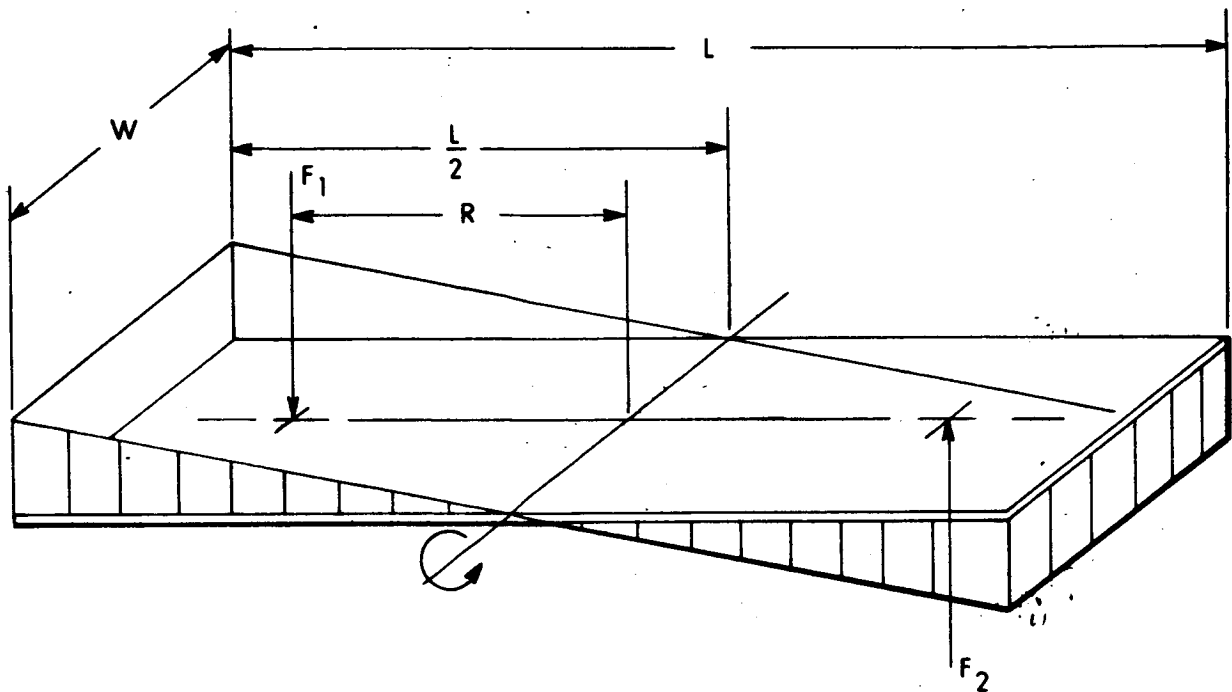


Figure 4-1. Torsional Wind Loading Condition on the Solar Panel Worst Case Condition

where:

$$\begin{aligned}
 L &= 104 \text{ in.} \\
 L/2 &= 52 \text{ in.} \\
 R &= 34.6 \text{ in.} \\
 W &= 54 \text{ in.} \\
 A &= 2808 \text{ in}^2 \quad (19.5 \text{ ft}^2)
 \end{aligned}$$

The total moment is:

$$M_t = 2(M) = 1478 \text{ in-lb}$$

The maximum shear stress,  $S_s$  is found by the equation:

$$S_s = \frac{M_t (16)}{\pi d^3 \left(1 - \frac{d_1^4}{d^4}\right)}$$

where:  $M_t = 1478 \text{ in-lb}$   
 $d = 2.000 \text{ in}$   
 $d_1 = 1.960 \text{ in}$

Therefore

$$\begin{aligned} S_s &= \frac{1478 (16)}{\pi (2.000)^3 \left(1 - \frac{1.960^4}{2.000^4}\right)} \\ &= 12,200 \text{ psi} \end{aligned}$$

The margin of safety of the rotating boom is:

$$\text{M.S.} = \frac{S_{cr}}{S_s (\text{FS})} - 1$$

The allowable stress based on elastic buckling of the thin walled torque tube is:

$$S_{cr} = 0.272 \frac{E}{(1 - \nu^2)^{3/4}} \left(\frac{2t}{d}\right)^{3/2}$$

(See Roark, formulas for stress and strain)

$E = 42 \times 10^6$   
 $\nu = 0.01$   
 $t = 0.020$   
 $d = 2.00$

$$S_{cr} = \frac{(0.272)(42)(10^6)(0.002825)}{(0.924)}$$

$$S_{cr} = 34,931 \text{ psi}$$

The allowable buckling stress is lower than the shear strength of the material and therefore determines the margin of safety for the tube

$$M.S. = \frac{34,930}{12,200 \times 1.25} - 1$$

$$M.S. = 1.25$$

The rotational deflection of the tube is given by:

$$\theta = \frac{ML}{KG}$$

where:  $M = 1478 \text{ in-lb}$

$L = 120 \text{ in}$

$K = 1/2\pi r^3 t = 0.0314$

$r = 1.0$

$t = 0.020$

$G = \text{Shear Modulus} = 20 \times 10^6 \text{ psi}$

$$\theta = \frac{(1478)(120)}{(20 \times 10^6)(0.0314)} = 0.281 \text{ rad} = 16.1^\circ$$

#### CONCLUSION

Further analysis of this configuration will require determination of the tolerable rotational deflection of the deployed panels and the development of a more refined wind loading condition. The rotating boom will be sized by deflection criteria rather than strength. The possibility of using a composite material for the torque tube should be investigated.

#### 4.2.2 SUPPORT TRUSS

The truss which supports the rotating boom is shown schematically in Figure 4-2. The truss is designed to use beryllium tubes fabricated from cross-rolled sheet.

Each solar panel section is latched to the spacecraft body during launch so that the effective dead load on the support truss in the Z direction is as summarized below:

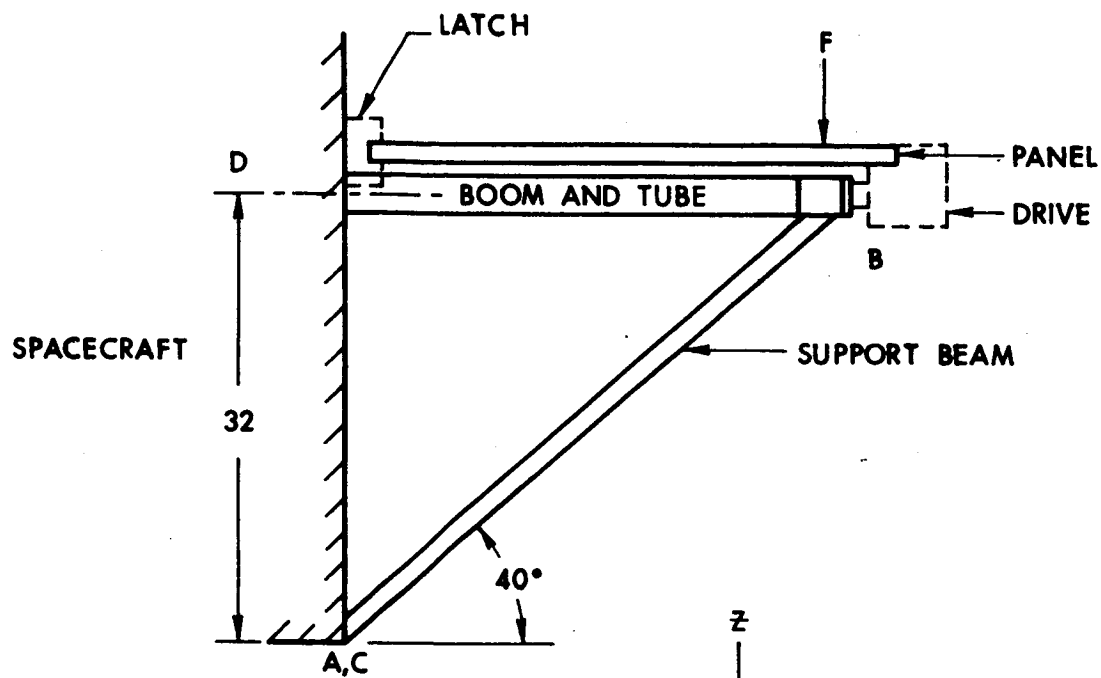
Panel - 9.20 (0.5)	= 4.600
Rotating Boom (0.45) (0.5)	= 0.275
Motor	0.500
Bearings	0.200
Gear Drive	1.000
Horizontal Tube (0.546)(0.5)	0.273
Diagonal Tubes	<u>0.413</u>
F = 7.061	

The fundamental resonant frequency of the support truss can be estimated from the following relation

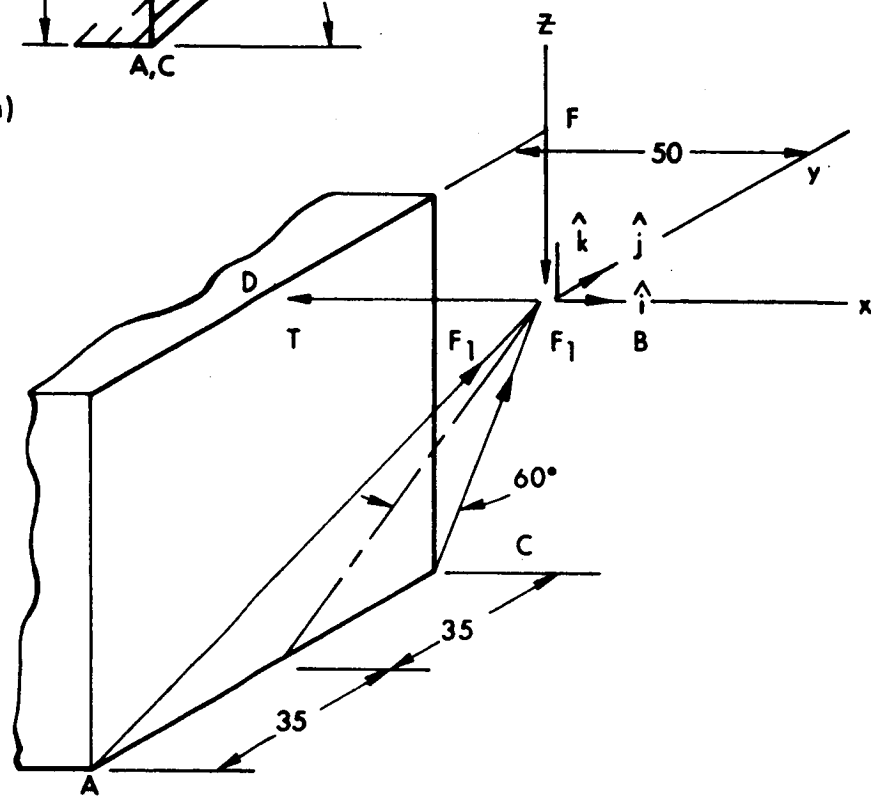
$$f_n = \frac{1}{2\pi} \sqrt{\frac{g}{D_z}}$$

where  $D_z$  is the vertical static displacement produced by the effective dead load.  $D_z$  is determined as shown below.

$$\begin{aligned} \vec{F}_{AB} + \vec{F}_{CB} + \vec{F}_{DB} + \vec{F} &= 0 \\ \vec{F}_{AB} &= \frac{F_{AB}}{68.913} (50 \hat{i} + 35 \hat{j} + 32 \hat{k}) \\ \vec{F}_{CB} &= \frac{F_{CB}}{69.913} (50 \hat{i} - 35 \hat{j} + 32 \hat{k}) \\ \vec{F}_{DB} &= F_{DB} (\hat{i}) \quad F = -7.061 \hat{k} \end{aligned}$$



a)



b)

Figure 4-2. Launch Loading Conditions on the Support Truss

$$\begin{bmatrix} 50 & 50 & 68.913 \\ 35 & -35 & 0 \\ 32 & 32 & 0 \end{bmatrix} \begin{bmatrix} F_{AB} \\ F_{CB} \\ F_{DB} \end{bmatrix} = \begin{bmatrix} 0 \\ 0 \\ 7.061 \times 68.913 \end{bmatrix}$$

$$F_{AB} = \frac{\begin{bmatrix} 0 & 50 & 68.913 \\ 0 & -35 & 0 \\ (7.061)(68.913) & 32 & 0 \end{bmatrix}}{2(68.913)(32)(35)} = \frac{(68.913)^2 35 (7.061)}{2(68.913)(32)(35)}$$

$$F_{AB} = \left( \frac{68.913}{64} \right) (F) = 1.07676F = (1.07676)(7.061) = 7.60$$

$$F_{CB} = F_{AB} = 7.60 \text{ lb}$$

$$F_{DB} = \frac{-(7.061)(68.913)(2)(35)(50)}{2(68.913)(32)(35)}$$

$$F_{DB} = \frac{-50}{32} (7.061) = 1.5625F = 11.033 \text{ lb}$$

$$F_{BD} = 11.033 \text{ lb}$$

#### TABULATION OF CALCULATION OF VERTICAL DEFLECTION $D_x$

Member	Area, A Sq. in.	Length, L in.	F lb	$e = \frac{FL}{AE}$	Unit Load, $P_Z$ lb/lb	$P_Z e$ in.
AB	0.100	68.913	-7.60	-.000125	-1.0768	.000135
BC	0.100	68.913	-7.60	-.000125	-1.0768	.000135
BD	0.176	50	11.033	.000074	1.5625	.000116

$$D_Z = \Sigma P_Z e = .000386$$

The natural frequency is:

$$f_n = \frac{1}{2\pi} \sqrt{\frac{386}{0.000386}} = \frac{10^3}{2\pi}$$

$$f_n = 159.1 \text{ Hz}$$

From Figure 4-3, the input acceleration for main structure at 160 Hz is 5 g (0-peak).

Applying a 5 g input with a Q of 20 gives the following dynamic loads in the truss members

$$F_{AB} = F_{CB} = 760 \text{ lb}$$

$$F_{BD} = 1103 \text{ lb}$$

These loads are alternating tension-compression loads.

The critical loads for Euler buckling are given by:

$$F_{CR} = \frac{\pi^2 EI}{l^2}$$

$$F_{CR(AB)} = \frac{\pi^2 (42)(10^6) (\pi)(1)^3 (0.016)}{(68.913)^2}$$

$$F_{CR(AB)} = 4387 \text{ lb}$$

Member BD is less critical than members AB and CD. The margins of safety on Euler buckling are high. ( $> 4$ ) for three members of the truss.

The local resonant frequency of the diagonal members of the truss is:

$$f_n = 1.57 \sqrt{\frac{EI}{\rho L^4}}$$



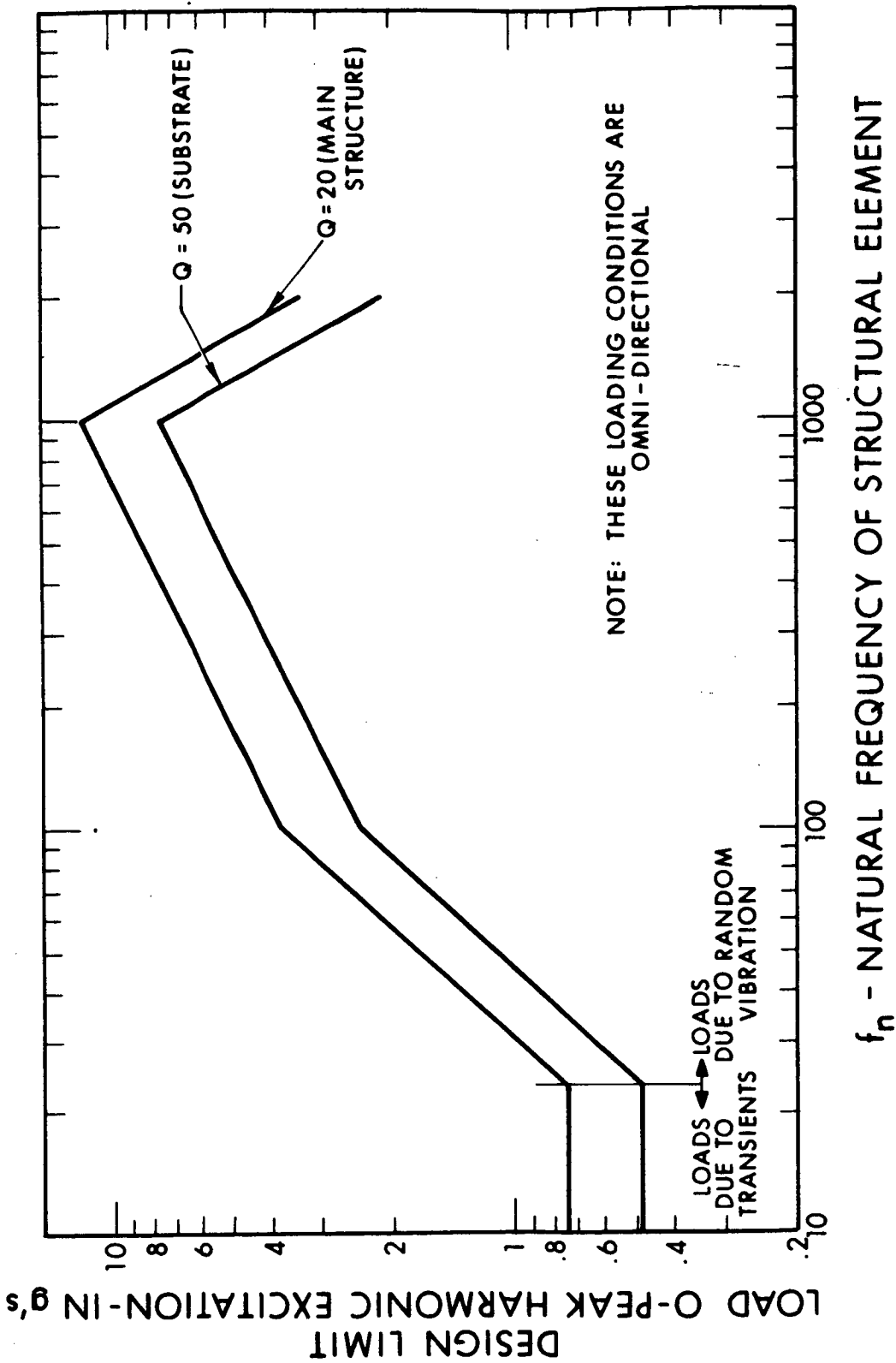


Figure 4-3. Design Loads for Launch Configuration

where:  $E = 42 \times 10^6$  psi

$$I = \pi R^3 t = 0.0503$$

$$\rho = \frac{0.079}{g} \frac{lb}{ft} = 1.7055 \times 10^{-5} \frac{lb \text{ sec}^2}{in.^2}$$

$$L = 68.913 \text{ in.}$$

$$f_n = \frac{1.57 \times 10^3}{4749} \sqrt{\frac{42 (.0503)}{1.7055 \times 10^{-5}}}$$

$$f_n = 33.059 \sqrt{12.387}$$

$$f_n = 116.333 \text{ Hz}$$

The input at this frequency is 4.6 g's (0-peak).

The maximum bending moment in the beam due to the local resonance is:

$$M = \frac{4}{\pi^3} \ddot{\delta}_s \rho Q L^2$$

$$\ddot{\delta} = (4.6)(386)$$

$$Q = 20$$

$$M = \frac{4}{\pi^3} (4.6)(386)(1.7055 \times 10^{-5})(20)(4749) = 370.9 \text{ in-lb}$$

The bending stress is

$$S = \frac{Mc}{I} = \frac{(370.9)(1)}{0.0503} = 7,375. \text{ psi}$$

The margins of safety on yield and buckling for this loading condition are high.

## SECTION 5

### SYSTEM ANALYSIS

- 5.1 ENVIRONMENTAL INTERACTION (see Volume I)
- 5.2 MATERIALS EVALUATION (see Volume I)
- 5.3 THERMAL ANALYSIS - FLAT PANELS

Temperature estimates for an oriented array are presented for six cases in Table 5-III. The assumed background temperatures are given in Table 5-IV. Heat balance equations and assumptions are given below.

Since the presence of atmospheric convection is felt primarily as a leveling influence, an approximation which ignores convection is conservative. All the oriented arrays reach a maximum temperature when they are normal to the sun vector. The range of Mars surface influence can be spanned by assuming a panel perpendicular to the Mars surface (both sides see the surface, and both sides the sky) and parallel (the cell side sees only sky, the back side only the surface of Mars). A heat balance for the vertical panel gives the following solution:

$$\sigma T^4 = \frac{FG_s [\alpha_{s1}(1 - \eta) + \bar{S}A_m (\alpha_{s1} + \alpha_{s1})] + (1 - t) \epsilon \sigma T_a^4 + \epsilon \sigma T_m^4}{2\epsilon} \quad (1)$$

and for a horizontal array:

$$\sigma T^4 = \frac{FG_s [\alpha_{s1}(1 - \eta) + \bar{A}_m \alpha_{s2}] + (1 - t) \epsilon \sigma T_a^4 + \epsilon \sigma T_m^4}{2\epsilon} \quad (2)$$

Terms are defined in Table 5-V. For a best average estimate, vertical panels were assumed at dawn and sunset, and horizontal panels at noon. The effects of shadowing, spacecraft interaction, or dust storms have not been included.

TABLE 5-III  
TEMPERATURE ESTIMATES

	<u>First Day of Spring, Equator</u>	<u>First Day of Summer, 20°N Latitude</u>
Dawn	10.1°C	0.2°C
Noon	24.6°C	15.3°C
Sunset	20.5°C	11.0°C

TABLE 5-IV  
ASSUMED BACKGROUND TEMPERATURES

	<u>First Day of Spring, Equator</u>	<u>First Day of Summer, 20°N Latitude</u>
Solar Constant ( $G_s$ )	60 mW/cm <sup>2</sup>	50 mW/cm <sup>2</sup>
Average Sky Temperature	220°K (-53°C)	208°K (-65°C)
Dawn Temperature	240°K (-33°C)	238°K (-35°C)
Noon Temperature	285°K ( 12°C)	281°K ( 8°C)
Sunset Temperature	270°K ( -3°C)	267°K ( -6°C)

TABLE 5-V  
TABLE OF NOMENCLATURE

$\sigma_{s1}$	= solar absorptivity cell side = 0.81
$\sigma_{s2}$	= solar absorptivity back side = 0.30 (white paint)
F	= transmission factor to sunlight = 0.92
$G_s$	= solar constant at Mars orbit
$\eta$	= solar panel efficiency
$\bar{A}_m$	= Mars surface albedo
$F_{1-m}$	= cell side view factor of Mars surface
t	= atmospheric transmissivity to Mars radiation = 0.90
$\sigma$	= Boltzmann's Constant, $36.6 \times 10^{-12} \text{ w/in}^2 \text{ } ^\circ\text{K}^4$
$T_1$	= cell side temperature
$T_a$	= sky temperature
$T_m$	= surface and ambient atmosphere temperature
h	= heat transfer coefficient, watts/in. $^\circ\text{C}$ (reference: first quarterly report)
C	= conductance of solar panel
$T_2$	= back side surface temperature

#### 5.4 WEIGHT ANALYSIS, TWO PANEL ORIENTED ARRAY

The weight breakdown for the two panel oriented array is given in Table 5-VI.

#### 5.5 RELIABILITY CONSIDERATIONS FOR THE TWO AXIS HORIZONTALLY MOUNTED ARRAY

##### 5.5.1 PHYSICAL DESCRIPTION

The array consists of two individual solar panels deployed as shown in drawing 7254-116, refer to Fig. 2-1. Each of the two panels electrically consists of submodules having six parallel cells each. A total of 60 submodules are series connected to form one section. Twenty sections are parallel connected to provide the required power output per panel. To provide electrical isolation between panel and output load, a pair of redundant diodes are connected to the output of each section. The purpose is to provide protection to the satellite power system in event of a short to the substrate of any section. The probability of a failure mode of this type occurring is minimal.

##### 5.5.2 RELIABILITY DEFINITION

The array electrical reliability is defined as the probability that the panel will produce a minimum of 200 watts at noon during the Martian summer season with the panels correctly positioned (perpendicular to the sun vector).

Spring/fall conditions are such that panel output will increase 12% over the summer season.

TABLE 5-VI  
WEIGHT ANALYSIS

Item	Description	Weight/Unit		No. of Units	Total Wt. (lb)
		Calc.	Est.		
I. Solar Panel					
A. Mechanical					
1. Substrate	Aluminum hollow core - 1.25 in. Holes 4 mil skin	0.035 lb/ft <sup>2</sup>		75.7 ft <sup>2</sup>	2.650
2. Beams	Beryllium - 2 in. diam 0.010 in. wall	0.05 lb/ft		52.6 ft	2.630
3. Hinge fittings	Titanium		0.10	4	0.400
4. Attachment clip	Aluminum extrusion	0.012 lb/ft		52.6 ft	0.632
5. Dielectric film	Kapton H-film, 1 mil	0.0072 lb/ft <sup>2</sup>		75.7 ft <sup>2</sup>	0.545
					6.857
B. Adhesives (Mech.)					
1. H-film to substrate	2 mil Narmco 3135 - 18% area	0.0103 lb/ft <sup>2</sup>		13.6 ft <sup>2</sup>	0.140
2. Substrate to clip	10 mil	0.04 lb/ft <sup>2</sup>		0.55 ft <sup>2</sup>	0.022
3. Clip to beam	10 mil	0.04 lb/ft <sup>2</sup>		0.55 ft <sup>2</sup>	0.022
4. Beam to fitting	10 mil	0.04 lb/ft <sup>2</sup>		0.55 ft <sup>2</sup>	0.022
					0.206
C. Electrical					
1. Solar cell	10 mil, 2 x 2 cm, n-p silicon	5.35 x 10 <sup>-4</sup> lb/cell		14,400 cells	7.700
2. Coverglass	Tedlar film	5.0 x 10 <sup>-5</sup> lb/in <sup>2</sup>		9,200 in <sup>2</sup>	0.460
3. Interconnections		2.2 x 10 <sup>-5</sup> lb/unit		14,400 cell	0.317
4. Terminals		7.71 x 10 <sup>-4</sup> lb/unit		80	0.061
5. Diodes		0.001 lb/unit		80	0.080
6. Cabling		0.0029 lb/ft		40 ft	0.116
					8.734

TABLE 5-VI  
WEIGHT ANALYSIS (contd)

<u>Item</u>	<u>Description</u>	<u>Weight/Unit</u>		<u>No. of Units</u>	<u>Total Wt. (lb)</u>
		<u>Calc.</u>	<u>Est.</u>		
D. Adhesives (Elec.)					
1. Solar Cells	4 mil RTV 41	1.1 x 10 <sup>-4</sup>	1b/cell	14,400	1.585
2. Coverglass	Dow Corning XR-63489	4.4 x 10 <sup>-5</sup>	1b/cell	14,400	<u>0.634</u>
					2.219
				Subtotal	18.016
Main Beam	Beryllium - 170 in. long 2 in. o.d. x 0.016 wall	0.097	1b/ft	1	1.372
Support Bracing	Beryllium - 64 in. long 2 in. o.d. x 0.016 wall	0.079	1b/ft	4	1.655
Brace Fittings	Titanium	0.2		4	0.800
Support Tube	Beryllium 48 in. lg x 3 1/2 diam x 0.016 wall	0.1365	1b/ft	2	1.092
Panel Tilt Drive	Yoke and worm gear	1.0		2	2.000
Drive Motors		0.5		3	1.500
Rotation Drive	Boom rotation	0.75		1	0.750
Boom Bearings	Bearings and housing	0.2		4	0.800
Latches	Stowed lockup	0.2		4	0.800
Sun Sensors		0.1		4	0.400
Electronics	Orientation tracking	1.00		1	1.000
				Subtotal	12.169
				Total	30.185



### 5.5.3 POWER CAPABILITY

The expected array power (summer) will vary depending on the degree of panel shadowing encountered. With no shadowing, the expected output will be 274.2 watts. Under worst case shadowing (10 sections), output will be 205.7 watts.

The output during the spring/fall season will vary between 312.5 and 234.4 watts under the same operating conditions.

### 5.5.4 FAILURE MODE DISCUSSION

#### 5.5.4.1 Solar Cells

The critical mode for the cell array, in terms of power loss, is the open cell or cells that cause current limiting in the section containing the open units.

Shorted cells have less effect on the section power loss due to lack of the current limiting effect. As an example, the current loss due to a single open cell in one section will reduce the section power by approximately 7.5% and the total array output by 0.19%, whereas a single shorted cell will reduce the section power by a maximum of 1.7% and the overall array output by 0.04%.

#### 5.5.4.2 Diodes

The array will function with shorted diodes under normal operational situations. Parallel redundant diodes will be used in all sections and each diode is capable of handling the section load current. Therefore, the critical mode is the probability of more than one diode opening in a section during the mission.

#### 5.5.5 ANALYSIS

This analysis is based on the maximum number of electrical sections that may be rendered inoperative and still permit the array to meet the minimum power requirements for mission accomplishment. Since the degree of panel shadowing will affect the probability values, the calculations have been based on the assumption that a 50% shadowing condition exists (i.e., 5 sections).

##### 5.5.5.1 Failure Rates

The failure rates are:

$$\begin{aligned}\text{Solar cell} &= 0.01/10^6 \text{ hours} = \lambda_c \\ \text{Diode} &= 0.02/10^6 \text{ hours} = \lambda_d\end{aligned}$$

The cell failure rate is based on the value used for the EOS 770 program for a 2 x 2 cm cell. The diode failure rate is that used for the Surveyor solar panels built by EOS. Operational mission time = 8760 hours.

##### 5.5.5.2 Calculations

###### 5.5.5.2.1 Permissible Section Failures

Assuming five sections are shadowed, the additional section loss is calculated as:

$$\text{Maximum allowable power loss} = 239.9 - 200 = 39.9 \text{ watts}$$

$$\text{Nominal section power} = 6.86 \text{ watts}$$

$$\text{Allowable section failures} = \frac{39.9}{6.86} = 5 \text{ sections}$$

#### 5.5.5.2.2 Diode Reliability

$$\text{Single Diode } (R_D) = e^{-\lambda_D t} = e^{-(0.02 \times 8760 \times 10^{-6})}$$

$$R_D = 0.9998$$

$$\text{Redundant diodes } (R_{DR}) = 1 - (1 - R_D)^2$$

$$R_{DR} = 1 - (1 - 0.9998)^2 > 0.99999$$

#### 5.5.5.2.3 Cell Section Reliability ( $R_{SC}$ )

Assuming worst case\* conditions (no cell failures), the cell section reliability will be:

$$R_{SC} = e^{-N\lambda_{et}} e^{-(360 \times 0.01 \times 8760 \times 10^{-6})}$$

$$R_{SC} = 0.96895$$

#### 5.5.5.2.4 Total Section Reliability ( $R_S$ )

$$R_S = R_{DR} \times R_{SC} = 0.99999 \times 0.96895$$

$$R_S = 0.96894$$

#### 5.5.5.2.5 Total Array Reliability ( $R_A$ )

Assuming the 50% shadowing condition and the allowable section loss of 5 watts, the array reliability is obtained by expanding the first six terms of the binomial distribution.

---

\*This assumes complete loss of the section output due to a cell failure. In practice, the output will be degraded by a maximum of 7.5%.

$$R_A = \sum_1^6 (P + q)^N$$

$$R_A = \sum_1^6 (0.96894 + 0.0316)^{35}$$

$$R_A = 0.99944$$

SECTION 6  
PRELIMINARY MANUFACTURING PLAN

(Refer to Volume I)

## SECTION 7

### PRELIMINARY TEST PLAN

#### 7.1 INTRODUCTION

This section describes the test program proposed for qualifying the JPL/SPA two panel, oriented array for the environments of sterilization, storage and transportation, launch, flight, Mars landing, and one Earth year on the Martian surface. Included are tests of components where they represent substantial innovations and tests to be performed during fabrication to determine acceptability of subassemblies. Additional tests not listed will be performed as required to qualify materials and manufacturing techniques.

We have developed a large body of special techniques for the testing of solar panels, many of which will have direct application to the JPL/SPA program.

##### 7.1.1 DEFINITIONS

- a. Substrate: Any one of two cell-supporting structures which compose each half of the cell array, without cells.
- b. Prototype Panel: Any one of the substrates with "dummy" cells or partial complement of "live" cells. To be used for testing purposes only, not for flight use.
- c. Qualification Panel: Any one of the substrates with "live" cells attached and in final flight configuration. To be used for testing purposes only, not for flight use.
- d. Flight Panel: Any one of the substrates with "live" cells attached and in final flight configuration. To be used for flight use.
- e. Test Module: A group of cells, 6P x 6S, electrically interconnected and mounted to substrate representative of the actual panel substrate but one foot square in size.

- f. Mounting Structure: One of two support structures and three orientation drive mechanisms, sharing a common main shaft tube. The support structures are identical, each supporting a flight panel during launch, flight, and landing in a stowed position, and supporting it in the orientated operating positions after landing.
- g. Solar Planetary Array or "Array": The complete power system as related to the flight panels and mounting structure.

## 7.2 SOLAR ARRAY TESTS

A summary of the test program is presented in Table 7-I.

TABLE 7-I

### TEST PROGRAM SUMMARY

<u>Table</u>	<u>Item</u>	<u>Qty</u>	<u>Test Description</u>
7-II	Test Module	4	Engineering Evaluation
7-III	Prototype Panel	1	Prototype Panel Test
7-IV	Prototype Array	1	Prototype Panel and Mounting Structure Test
7-V	Qualification Panel	2	Preliminary Flight Acceptance Test
7-VI	Qualification Panel	2	Formal Qualification Test
7-VII	Qualification Array	1	Formal Type Approval Test
7-VIII	Qualification Panel	1	Formal Reliability Test
7-V	Flight Panels	4	Flight Acceptance Test

#### 7.2.1 ENGINEERING EVALUATION TEST

This test shall be performed on 4 test modules consisting of 6P x 6S cells, each mounted on a square foot substrate representative of the flight substrate.

Performance and environmental testing shall be accomplished to establish advance confidence in fabrication techniques, testing, and environmental requirements prior to conducting prototype tests. Performance and environmental test data shall be recorded and maintained.

Table 7-II shows the testing sequence for each test.

TABLE 7-II

ENGINEERING EVALUATION TEST SEQUENCE

Item:	Test Module
Quantity:	Four
1.	Mechanical inspection
2.	Simulator test
3.	Application of cover film
4.	Mechanical inspection
5.	Simulator test
6.	Sterilization
7.	Mechanical inspection
8.	Simulator test
9.	Rapid decompression
10.	Mechanical inspection
11.	Simulator test
12.	Mars environment
	7 millibars pressure
	270 mph wind
	1 to 100 $\mu$ abrasive, conductive dust
13.	Mechanical inspection
14.	Simulator test
15.	Accelerated weathering
16.	Mechanical test
17.	Simulator test



### 7.2.2 PROTOTYPE TESTING

This test shall be performed in two parts: first, a prototype panel shall be tested per the testing sequence shown in Table 7-III, and then the panel shall be mounted to a prototype structure and tested for orientation capabilities in a wind tunnel to simulate the dynamic loading conditions per the test sequence shown in Table 7-IV.

TABLE 7-III

#### PROTOTYPE PANEL TEST

Item: Substrate, with dummy cells

Quantity: One

1. Mechanical inspection
2. Vibration (sinusoidal)
3. Mechanical inspection
4. Vibration (random)
5. Mechanical inspection
6. Sterilization
7. Mechanical inspection
8. Rapid decompression
9. Mechanical inspection
10. Temperature cycling
11. Mechanical inspection

TABLE 7-IV

PROTOTYPE PANEL AND MOUNTING STRUCTURE TEST

Item: Prototype array (one panel only)

Quantity: One

1. Mechanical inspection
2. Deployment - horizontal
3. Mechanical inspection
4. Deployment 34° upward
5. Mechanical inspection
6. Deployment 34° downward
7. Mechanical inspection
- 8 through 14. Repeat steps 2 through 7 in an 18.5 mph wind  
(1 atmosphere pressure)
- 15 through 21. Repeat steps 8 through 14 with wind from 90°  
direction

7.2.3 ACCEPTANCE TEST

Acceptance testing will be performed on all flight panels prior to delivery to JPL, and on the qualification panels prior to qualification testing. The electrical and environmental test data shall be recorded and maintained. All sunlight and rooftop tests include diode reverse leakage and insulation resistance tests.

EOS will perform the acceptance tests in the sequence shown in Table 7-V. The acceptance test will be performed on the qualification panel and on each panel of all flight units.

TABLE 7-V

ACCEPTANCE TEST SEQUENCE

To be performed on any flight panel.

1. Sunlight test
2. Acoustic test
3. Mechanical inspection
4. Rooftop test
5. Temperature cycling
6. Mechanical inspection
7. Sunlight test

7.2.4 QUALIFICATION TEST

To be performed on two solar panels.

All individual tests shall be performed without any adjustments and/or repairs being accomplished during such tests. In the event of a test failure, EOS will stop all further testing and shall not proceed before notifying JPL. All data taken during electrical and environmental testing shall be recorded and maintained.

Prior to any qualification testing, the solar panels shall have satisfactorily passed the electrical and environmental requirements of acceptance testing.

Table 7-VI shows the qualification test sequence.

7.2.5 FORMAL TYPE APPROVAL TEST

After completion of the individual qualification panel tests, these units shall be assembled to a complete mounting structure and a

TABLE 7-VI

## QUALIFICATION TEST SEQUENCE

To be performed on two solar panels.

1. Sunlight test
2. Relative humidity
3. Mechanical inspection
4. Rooftop test
5. Sterilization
6. Mechanical inspection
7. Sunlight test
8. Vibration - transverse axis (sinusoidal and random)
9. Mechanical inspection
10. Vibration - lateral axis (sinusoidal and random)
11. Mechanical inspection
12. Vibration - longitudinal axis (sinusoidal and random)
13. Mechanical inspection
14. Rooftop test
15. Shock  $\pm$  transverse axis
16. Mechanical inspection
17. Shock  $\pm$  lateral axis
18. Mechanical inspection
19. Shock  $\pm$  longitudinal axis
20. Mechanical inspection
21. Rooftop test
22. Acoustic
23. Mechanical inspection
24. Rooftop test
25. Temperature vacuum
26. Mechanical inspection
27. Rooftop test
28. Temperature cycling
29. Mechanical inspection
30. Rooftop test
31. Rapid decompression
32. Mechanical inspection
33. Sunlight test

simulated vehicle body for type approval testing. The testing shall be per the sequence shown in Table 7-VII.

TABLE 7-VII

TYPE APPROVAL TEST

Item:           Qualification Array

- a. Two qualification panels
- b. Qualification mounting structure

Quantity: One

1. Mechanical inspection
2. Sunlight test (panels)
3. Vibration - transverse axis (sinusoidal and random)
4. Mechanical inspection
5. Vibration - lateral axis (sinusoidal and random)
6. Mechanical inspection
7. Vibration - vertical axis (sinusoidal and random)
8. Mechanical inspection
9. Rooftop test
10. Shock (general)  $\pm$  transverse axis
11. Mechanical inspection
12. Shock (general)  $\pm$  lateral axis
13. Mechanical inspection
14. Shock (general)  $\pm$  vertical axis
15. Mechanical inspection
16. Rooftop test
17. Type approval system sterilization
18. Mechanical inspection
19. Rooftop test
20. Disassembly
21. Mechanical inspection
22. Sunlight test (panels)

#### 7.2.6 RELIABILITY TEST

EOS will perform the reliability test using one panel previously used during qualification testing.

The panel shall be subjected to a total of 30 days of environmental conditions. Every 120 hours the unit shall be removed from its environment and rooftop tested.

Table 7-VIII shows the test sequence for the reliability tests.

#### NOTE

If wind tunnel test of deployed array shows substantial vibration or oscillation, a reliability test may be required to evaluate this parameter.

TABLE 7-VIII

#### RELIABILITY TEST SEQUENCE

To be performed on one solar panel (used in qualification test sequence, above).

1. Sunlight test
2. Temperature cycle (5 days)
3. Rooftop test
4. Remperature cycle (same as 2)
5. Rooftop test (same as 3)
6. Temperature cycle (same as 2)
7. Rooftop test (same as 3)
8. Temperature cycle (same as 2)
9. Rooftop test (same as 3)
10. Temperature cycle (same as 2)
11. Rooftop test (same as 3)
12. Temperature cycle (same as 2)
13. Sunlight test (same as 1)

#### 7.2.7 SHIPPING CONTAINER TEST

The test shall consist of three drops from an elevation of 12 inches. The container shall be dropped once in each plane as follows:

- a. Flat
- b. Edgewise (long edge)
- c. Edgewise (short edge)

The object of these tests is to determine that no physical damage occurs to the SPAs which may be in the container. All data shall be recorded and maintained.

#### 7.3 TEST EQUIPMENT AND FIXTURES

EOS has maintained the latest in test equipment to record and resolve data within the parameters of present day requirements.

Three basic means of data acquisition for performance testing of solar devices are employed: digital voltmeters, digital printers, and X-Y recorders. Sun simulators are used to illuminate some of the solar devices; these will be discussed later.

The latest in test equipment is employed for environmental requirements. Digital voltmeters, temperature recorders, and electronic control equipment are a few of those utilized for controlling, resolving, and recording data and/or functions. Presently being used are environmental chambers capable of reaching pressures of  $1 \times 10^{-6}$  torr and simulating space environment conditions of solar panel testing.

Fixtures for vibration and shock, acoustic, temperature cycling, humidity tests, and altitude temperature tests will be specially designed.

#### 7.4 PERFORMANCE TESTING (Sunlight, Rooftop, and Solar Simulator)

EOS will make performance tests for the purpose of acceptance during fabrication levels and final acceptance. The following paragraphs discuss the individual tests in greater detail.

##### 7.4.1 SINGLE CELL TESTING

Individual cell measurements will be made under a tungsten iodine light source, calibrated to an intensity of  $140 \text{ mW/cm}^2$  (AMO). A standard cell, typical in spectral response to cells being fabricated into SPAs, shall be calibrated against a JPL balloon flown standard.

##### 7.4.2 SUBMODULE TESTING

The submodule testing is performed under the same tungsten iodine simulator discussed in Subsection 7.4.1.

The submodules are tested for  $I_{sc}$  (short circuit current) and the current at 485 mV. These tests are performed while the submodule is at a temperature of  $28^\circ \pm 2^\circ\text{C}$ . Calibration of the submodule area ( $2 \text{ cm} \times 12 \text{ cm}$ ) will be performed with a standard cell and set for an intensity of  $140 \text{ mW/cm}^2$ . Area uniformity will be held to within  $\pm 1\%$  or less.

The test fixture has the standard 4-point probe electrical contact system, and also employs a vacuum system to aid in securing the submodule to the base.

##### 7.4.3 SAMPLE MODULE TESTING

The  $6 \times 6$  cell sample module used in the test sequence of Table 7-II will be tested under a xenon solar simulator.



#### 7.4.4 PANEL TESTING

EOS will test the SPAs in sunlight. An I-V curve will be produced for each circuit on the panel and for a total panel.

"Sunlight" tests will be performed at Table Mountain, California.

"Rooftop" tests will be performed at the Pasadena facility.

The I-V plots will be drawn with an X-Y recorder and points ( $I_{sc}$  and  $V_{oc}$ ) will be checked against a digital voltmeter. Data acquired during testing (temperature, intensity, panel electrical outputs, date, time, etc.) will be properly recorded and maintained.

Sunlight performance tests are performed when the following conditions exist:

- Sky radiation 10 percent or less
- Sun intensity approximately  $100 \text{ mW/cm}^2$

Data obtained during testing of solar panels is extrapolated from AM1 ( $100 \text{ mW/cm}^2$ ) to AM0 ( $140 \text{ mW/cm}^2$ ).

Tests will be performed to determine the characteristic temperature response of the cells and that data will be used to derive panel open circuit voltage.

$I_{sc}$  corrections must be made to correct for sun intensity losses through the Earth's atmosphere. An equation for  $I_{sc}$  correction is as follows:

$$I_{scp_1} = I_{scp_2} \times \frac{I_{scuc}}{I_{scn}}$$

where:  $I_{sc1}$  = the corrected short circuit current for a circuit

$I_{sc2}$  = the recorded short circuit current for a circuit during testing

$I_{scuc}$  = the standard cell, uncollimated, short circuit current reading during testing

$I_{scn}$  = the calibrated AMO short circuit current for the standard cell

Extrapolations for  $I_{sc}$  and  $V_{oc}$  will be determined and a corrected I-V curve shall be replotted for an AMO ( $140 \text{ mW/cm}^2$ ) intensity. The maximum power point will then be determined from this curve.

## SECTION 8

### SUMMARY

This report finalizes the detailed analysis and demonstrates the feasibility of the second of three array concepts of a planetary photovoltaic solar array for operation on the Martian surface.

The system presented here is a two panel oriented array system meeting all the packaging constraints imposed on the design by JPL in drawing No. 1002-3236A. The basis of this concept was to present to JPL a system which had orientation capability, minimizing the shadow problem, without combining the antenna system with the solar panels. The design is a tradeoff against the antenna shadow problem in which the total array was sized at 40 circuits, instead of the minimum of 30 circuits required.

This system will meet the desired goal of 20 W/lb at 1 AU and exceed the minimum power of 200W at solar noon for worst case conditions. The actual power output will vary dependent upon the number of circuits that are possibly shadowed at noon. For the lowest solar intensity occurring at the first day of Martian summer (summer solstice) the power output limits are:

Max shadow (30 circuits) = 205.6W

No shadow (40 circuits) = 274.2W

For the higher solar intensities occurring at spring and fall seasons the power levels range from 234.4W to 312.5W, considerably over the minimum requirement.

A summary of the system is as follows:

- a. Type of cell - 0.010 thick, 2 x 2 cm, N/P, top contact, 1-3 ohm-cm, solderless
  - b. Output of cell - 58 mW at 485 mV (AMO)
  - c. Number of cells/circuit - 6P x 60S
  - d. Number of circuit/panel - 20
  - e. Number of panels/array - 2
  - f. Total number of cells - 14,400
  - g. Number of orientation drives - 3
  - h. Orientation mode - continuous motor gear drive, with solar cell sun sensors
  - i. Weight summary: (lb)
    - (1) Panels - 6.857
    - (2) Adhesives - 0.206 (structural)
    - (3) Structure and drive - 12.169
    - (4) Solar cells and components - 8.734
    - (5) Adhesives - 2.219 (cell mtg.)
- |       |           |
|-------|-----------|
| Total | 30.185 lb |
|-------|-----------|

The power to weight ratio, based on 1 AU, varies with the power output of the panels as a function of shadowing, as previously mentioned. For the lowest output condition of noon at the summer solstice with a solar intensity on the Martian surface of  $46 \text{ mW/cm}^2$  the specific power/weight ratios are:

Power at solar noon:

Min - 205.6W  
Max - 274.2W

Converting to 1 AU by the ratio of  $46/140 = 0.328$

$$205.6/0.328 = 626W$$

$$274.2/0.328 = 837W$$

Therefore, the specific power at 1 AU (AMO) would be:

$$626/30.185 = 20.8 \text{ W/lb}$$

$$837/30.185 = 28.6 \text{ W/lb}$$